Normal forms, bifurcations and finiteness properties of vector fields

Christiane ROUSSEAU

Département de mathématiques et de statistique and CRM
Université de Montréal
C.P. 6128, Succursale Centre-ville, Montréal (Qué.), H3C 3J7, Canada

October 2002

Abstract

These lectures make the bridge between the three themes of the book. Analytic objects have local finiteness properties. Compactness of the phase space and parameter space allows to derive global finiteness properties. One of the important tools for studying local properties is normal forms, which are also a tool to study bifurcations. In many generic situations the changes of coordinates to normal forms diverge. We explain this phenomenon in the case of a generic parabolic fixed point of a diffeomorphism by constructing a complete modulus of analytic classification of generic unfoldings of the diffeomorphism: the limit dynamics is too complicated to be encoded in the simple normal form. So the point of view of bifurcations brings a new light on the divergence of the normalizing series. Finally we recall the program to prove the finiteness part of Hilbert's 16th problem for quadratic systems started in 1991 and we discuss the progress of the program and what remains to be done.

Abstract

Short version for NATO These lectures make the bridge between the three themes of the book. Analytic objects have local finiteness properties. Compactness of the phase space and parameter space allows to derive global finiteness properties. One of the important tools for studying local properties is normal forms, which are also a tool to study bifurcations. In many generic situations the changes of coordinates to normal forms diverge. We explain this phenomenon in the case of a generic parabolic fixed point of a diffeomorphism by constructing a complete modulus of analytic classification of generic unfoldings of the diffeomorphism. Finally we recall the program to prove the finiteness part of Hilbert's 16th problem for quadratic systems started in 1991 and we discuss the progress of the program and what remains to be done.

This work is supported by NSERC and FCAR in Canada.

1 Introduction and perspectives

The text of this lectures makes the bridge between the three themes of the book. Although not exclusively, the main context will be analytic vector fields and analytic families of vector fields. The following ideas will be leading our mathematical developments:

- **Analytic objects have local finiteness properties.** In our context we will be mainly interested to the finite cyclicity of graphics of planar vector fields.
- **Compactness of the space phase yields to global finiteness properties.**
- **Compactness of the parameter space yields uniform finiteness properties.**

The main tools to study a vector field locally are:

(1) The flow-box theorem in the neighborhood of a singular point;

(2) Blow-ups and normal forms near singular points. We can consider blow-ups and normal forms of a single vector field as well as blow-ups and normal forms of families of vector fields.

Let us consider for a moment the problem of the finite cyclicity of graphics of planar vector fields. The standard method is to "calculate a return map" and to show that it has a finite number of fixed points. This return map can be written as a composition of regular transitions and Dulac maps in the neighborhood of the singular points. In the very generic situations, rough normal forms are sufficient to conclude to finite cyclicity, while in the more degenerate cases more refined normal forms are needed. For instance to prove the finite cyclicity of a homoclinic point through a saddle with nonzero trace (i.e. of codimension 1) a C^1 normal form is sufficient to conclude that the homoclinic loop has cyclicity one. When however we consider homoclinic loops of higher codimension more refined normal forms are needed. C^k normal forms are sufficient to treat the generic cases while analycity arguments are needed to treat the homoclinic loops with identity return map inside finite parameter analytic families of vector fields.

Let us consider a family $(v_\lambda)_{\lambda\in\Lambda}$ of vector fields with $v_{\lambda_0}(x_0) = 0$. A general principle which we want to push further is the following: **The most generic v_{λ_0} is, the most we know about v_λ in the neighborhood of x_0 for λ near λ_0.** As an example we can consider a vector field v_{λ_0} with two pure imaginary eigenvalues at x_0 and such that the first Lyapunov quantity is negative. Then we know that v_λ has none (resp. exactly one) limit cycle in the neighborhood of x_0 for values of λ for which the singular point x_λ (such that $x_{\lambda_0} = x_0$) is attracting (resp. repelling). If however the first $k-1$ Lypaunov quantities vanish and the k-th Lyapunov quantity is nonzero many more phase portraits are allowed. Finally when v_{λ_0} has a center at the origin the only thing we can say on x_λ is that it is a monodromic singular point.

The subject of normal forms was started by Poincaré and normal forms have been studied extensively since. If the singular points are not too degenerate reasonably good results exist for:

- formal normal forms;
- C^∞ normal forms for a single vector field;
- C^k normal forms for families of vector fields.

What about analytic normal forms?

i) They are the tools for problems of analytic classification under analytic changes of coordinates.

ii) Understanding the analytic type of a vector field in the neighborhood of an elementary singular point is an essential ingredient of the proof by Ecalle and Ilyashenko of the Dulac conjecture, namely that a polynomial vector field has a finite number of limit cycles.

iii) In many situations formal normalizing changes of coordinates diverge.

Some examples of orbital normal forms for which the formal normalizing change of coordinate can be divergent:

(1) The resonant saddle:

$$\begin{aligned} \dot{x} &= x(1+au^k) \\ \dot{y} &= y(-\tfrac{p}{q}+(1-a)u^k) \end{aligned} \tag{1.1}$$

where $u = x^p y^q$ is the resonant monomial.

(2) The saddle-node of codimension n:

$$\begin{aligned} \dot{x} &= x^{n+1} \\ \dot{y} &= \pm y(1+ax^n). \end{aligned} \tag{1.2}$$

(3) The non resonant saddle:

$$\begin{aligned} \dot{x} &= x \\ \dot{y} &= -\lambda y \end{aligned} \tag{1.3}$$

where λ is a Liouvillian irrational positive number.

(4) The diffeomorphism $f : (C,0) \to (C,0)$ with a parabolic fixed point:

$$f(z) = z + z^{n+1} + o(z^n+1). \tag{1.4}$$

The common point to all these situations is that **divergence is the rule and convergence is the exception**. Such systems have been studied thoroughly for fixed values of the eigenvalues or of the multiplier: they form natural "families" of systems. In a series of papers by Ilyashenko [19], [20]) we find theorems of the form: *Either the change of coordinates to normal form converges for all systems in the family or it diverges for the majority of systems (for almost all systems in the case of finite parameter families of systems).* Later, in the resonant cases, Ecalle [13] has given a more precise description of the subspace of parameter space where we can expect convergence.

As mentioned above in all these situations divergence is the rule and convergence is the exception. The question we want to consider is:

"WHY?"

The answer proposed is in the following spirit: our normal form is a kind of "model".

- Divergence is the rule and convergence is the exception **because the "model" is to poor to encode the rich dynamics of the system.**
- So the rich dynamics is encoded in the divergent normalizing transformation. **How to read it?**
- If we can read this rich dynamics it will become obvious that the poor dynamics of the model is an exceptional case.
- If divergence is the generic situation then, by the principle described above, we should expect to be able to describe some properties of local perturbations of the system.

Let us go back in the past and look at the following citation of Abel [1] (Œuvres complètes de Niels Henrik Abel, tome 2, in the letters to Holmboe, pages 256-257): *"Les séries divergentes sont en général quelque chose de bien fatal et c'est une honte qu'on ose y fonder aucune démonstration. On peut démontrer tout ce qu'on veut en les employant, et ce sont elles qui ont fait tant de malheurs et qui ont enfanté tant de paradoxes. ... Enfin mes yeux se sont dessillés d'une manière frappante, car à l'exception des cas les plus simples, par exemple les séries géométriques, il ne se trouve dans les mathématiques presque aucune série infinie dont la somme soit déterminée d'une manière rigoureuse, c'est-à-dire que* **la partie la plus essentielle des mathématiques est sans fondement.** *Pour la plus grande partie les résultats sont justes il est vrai, mais c'est là une chose bien étrange. Je m'occupe à en chercher la raison, problème très intéressant.*

The author has been fascinated by this complete change in the dynamics of the subject: Nowadays divergent series occupy a marginal place inside mathematics and we remember Abel as a mathematician who banished the use of divergent series.

To study why generically so many series diverge the point of view which is taken here is to **unfold**: the bifurcation point of view will help us understand the normal forms. Indeed many situations where we encounter divergence are limit situations, for instance:

i) Irregular singular points of linear differential equations occur when regular points coallesce.

ii) A parabolic point of a diffeomorphism of $(C, 0)$ is a fixed point of multiplicity $n + 1 > 1$.

iii) A saddle-node is a multiple singular point.

iv) The holonomy of a separatrix of a non integrable resonant saddle has a parabolic fixed point (hence a multiple fixed point) at the origin.

In these lectures we will address the following questions:

Questions:

(1) If the change of coordinates to normal form near x_0 diverges for v_{λ_0} (i.e. we are in the generic situation):

- what can we say of v_λ in the neighborhood of x_0 for λ close to λ_0? (We look for the properties which depend only on the germ of v_{λ_0} at x_0.)
- What analytic families v_λ can unfold v_{λ_0}? More precisely can we give the moduli space of the space of such analytic families?

(2) Can we understand the dynamics of v_{λ_0} from the fact that it is the limit of the v_λ for $\lambda \to \lambda_0$?

Let us illustrate this on an example:

The saddle-node: By an analytic change of coordinates we can bring an analytic system with a saddle-node of multiplicity 2 to the normal form:

$$\begin{aligned} \dot{x} &= x^2 \\ \dot{y} &= y(1+ax) + x^2 R(x,y). \end{aligned} \tag{1.5}$$

The formal normal form is our "model" (Figure 1a):

$$\begin{aligned} \dot{x} &= x^2 \\ \dot{y} &= y(1+ax). \end{aligned} \tag{1.6}$$

One obstruction to bring (1.5) to (1.6) is the non-existence of an analytic center manifold. We now unfold: the "model family" for the unfolding is (Figure 1b)

$$\begin{aligned} \dot{x} &= x^2 - \epsilon \\ \dot{y} &= y(1+a(\epsilon)x). \end{aligned} \tag{1.7}$$

To understand the dynamics we need to consider $x, y \in C$. Figure 2 represents the model and model family (only the x-variable is drawn as a 2-dimensional variable).

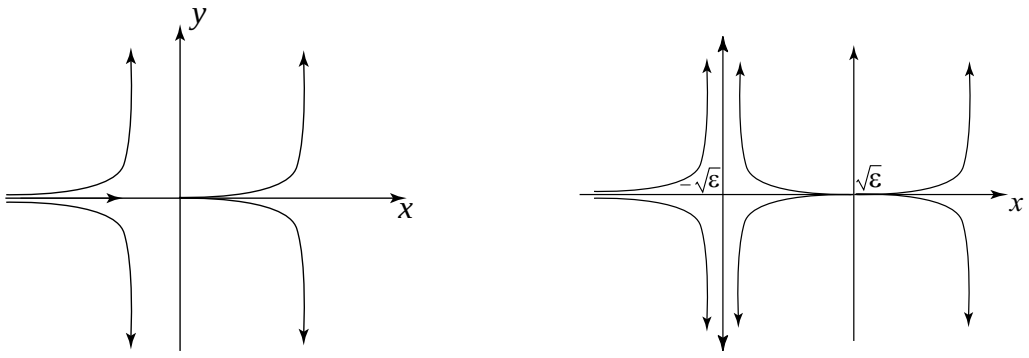

(a) $\epsilon = 0$ (b) $\epsilon \neq 0$

Figure 1: The "model"

Let us now suppose that (1.5) has no analytic center manifold. The formal equation of the center manifold

$$y = \sum_{n=2}^{\infty} b_n x^n \tag{1.8}$$

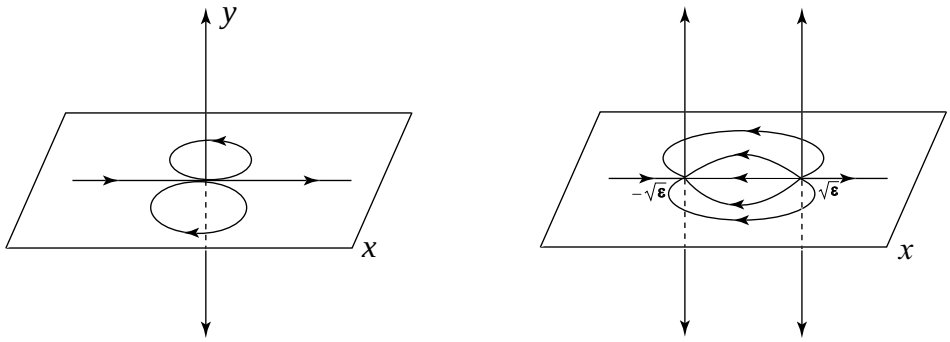

(a) $\epsilon = 0$ (b) $\epsilon \neq 0$

Figure 2: The "model"

is 1-summable in all directions except R^+ ([32]). This yields a "ramified" center manifold as in Figure 3a. To simplify we can suppose $a(\epsilon) \in R$, although this is not essential. Let now $\epsilon \in R^+$. The saddle point at $(-\sqrt{\epsilon}, 0)$ always has an invariant stable manifold which is necessarily ramified at the node as in Figure 3b.

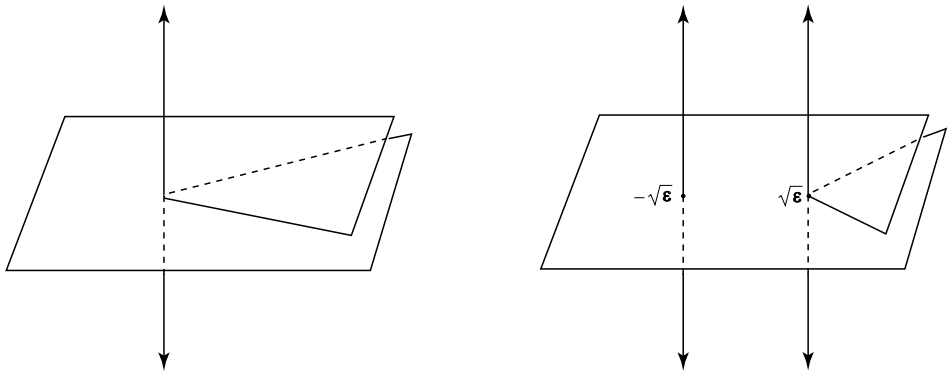

(a) $\epsilon = 0$ (b) $\epsilon \neq 0$

Figure 3: The invariant manifold

Let us now look at the local model at the node: it is known since Poincaré that the change of coordinates to the local model is always convergent. We have two cases:

- **Non resonant node:** the normal form is linear

$$\begin{aligned} \dot{x} &= \lambda x \\ \dot{y} &= y, \end{aligned} \tag{1.9}$$

when $\lambda \notin 1/N$. Integral curves (except the y-axis) have equation

$$y = Cx^{1/\lambda}. \tag{1.10}$$

Hence all integral curves are ramified except $x = 0$ and $y = 0$ which are analytic. The divergence of the series (1.8) yields that the analytic separatrices of the saddle and of the node do not glue together. Here **divergence means incompatibility** (Figure 4).

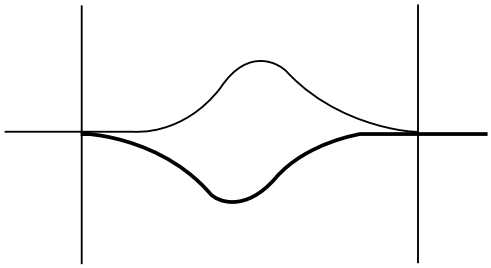

Figure 4: Incompatibility of the invariant analytic manifolds

- **Resonant node:** Here we have two cases. The exceptional case is when the node is linearizable

$$\begin{aligned} \dot{x} &= \tfrac{1}{n}x \\ \dot{y} &= y. \end{aligned} \tag{1.11}$$

In this case all integral curves (except $x = 0$) are of the form $y = Cx^n$. They are analytic, thus non ramified. Hence this case is necessarily excluded and we need be in the generic situation where the resonant monomial has a nonzero coefficient:

$$\begin{aligned} \dot{x} &= \tfrac{1}{n}x \\ \dot{y} &= y + bx^n, \end{aligned} \tag{1.12}$$

with $b \neq 0$. In this case the only non ramified integral curve is $x = 0$.

The conclusion is the following: **For some particular values of ϵ where one of the singular point is resonant the incompatibility implies some generic property of the unfolded point itself.** This observed phenomenon is very general: it is some form of *parametric resurgence*.

Similar resurgence phenomena occur at the saddle for parameter values for which it is resonant. We will learn to read them from the Martinet-Ramis modulus of analytic classification of the saddle-node.

We can of course extend to complex values of the parameter ϵ. When the ratio of the eigenvalues at $(\pm\sqrt{\epsilon}, 0)$ is not real the singular points are linearizable and have exactly two analytic trajectories, all other integral curves being ramified. If the saddle-node has no analytic center manifold then we observe in the unfolding that **the two (weak) analytic separatrices of $(\pm\sqrt{\epsilon}, 0)$ do not coincide.** This was already observed by Glutsyuk [15]. **But we can not make a full turn in the parameter space as $\sqrt{\epsilon}$ and $-\sqrt{\epsilon}$ are exchanged. We cannot expect a description of the phenomenon analytic in ϵ.**

The study of all these phenomena is done through the description of a complete modulus of analytic classification for generic analytic families unfolding a diffeomorphism with a generic parabolic point

$$f_\epsilon(z) = z + (z^2 - \epsilon)(1 + h(\epsilon, z)), \tag{1.13}$$

presented in detail in [33]. This allows to give an interpretation of all ingredients of the Ecalle-Voronin modulus of analytic classification of f_0.

1.1 The Ecalle-Voronin modulus of a generic diffeomorphism with a parabolic point

We describe the modulus of a germ of diffeomorphism

$$f_0(z) = z + z^2 + (1-a)z^3 + o(z^3). \tag{1.14}$$

The modulus is composed of three parts:

- *The discrete part* $k = 1$: $k+1$ is the multiplicity of the parabolic point. (Here we limit ourselves to the generic codimension 1 case.)
- *The formal part* $a \in C$: in the unfolding a is unfolded as $a(\epsilon)$ depending analytically of ϵ and is interpreted as a *shift* between the two singular points. Indeed the two singular points may not be resonant simultaneously.
- *The analytic part*: we describe precisely the diffeomorphism by describing its orbit space. The diffeomorphism is topologically equivalent to the time-one map of the flow of the vector field $z^2\frac{\partial}{\partial z}$ (see Figure 5).

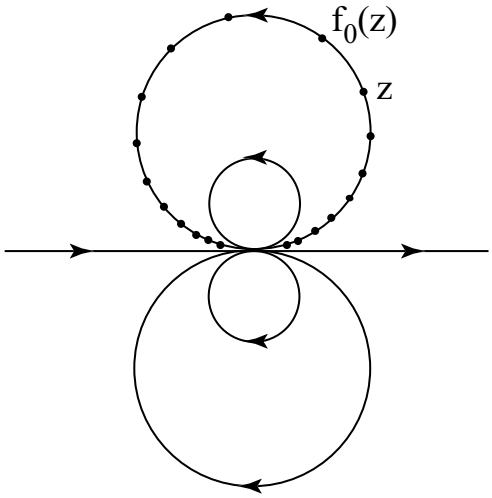

Figure 5: The diffeomorphism f_0

To describe the orbit space we give ourselves two "fundamental domains". To construct a *fundamental domain* we take a closed curve l through the origin such that $l \cap f_0(l) = \{0\}$. The fundamental domain is the domain between l and $f_0(l)$ where we identify l and $f_0(l)$ through $z \equiv f_0(z)$. Then each orbit has at most one point in a fundamental domain. There is no way to represent all orbits by a unique fundamental domain and two fundamental domains are necessary to represent the whole space of orbits. But then some orbits have representatives in the two fundamental domains. To describe the

orbit space we must identify points in the two fundamental domains which belong to the same orbit. This is done via a pair of maps defined respectively in the upper end and lower end of the fundamental domains (Figure 6).

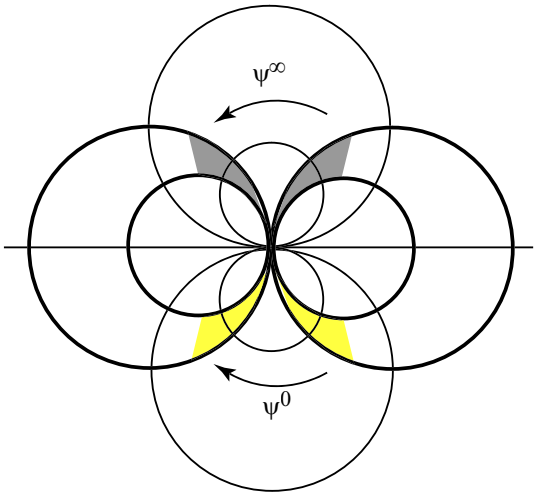

Figure 6: The two fundamental domains and identifying maps ψ^0 and ψ^∞

To describe these maps we use the fact that the fundamental domains are conformally equivalent to spheres $S^\pm$ with 0 and ∞ identified. Then there exist analytic diffeomorphisms $\psi^0, \psi^\infty : S^+ \to S^-$ defined in the neighborhood of 0 and ∞ such that the image of $w^+ \in S^+$ by ψ^0 or ψ^∞ is a point of S^- belonging to the same orbit as w^+. The diffeomorphisms ψ^0 and ψ^∞ are defined up to choices of coordinates on the spheres preserving 0 and ∞, i.e. up to composition by linear maps in the source and target space. Then

$$(\psi_1^0, \psi_1^\infty) \equiv (\psi_2^0, \psi_2^\infty) \quad \text{iff} \quad \exists C, C' \in C^* \begin{cases} \psi_1^0(w) = C\psi_2^0(C'w) \\ \psi_1^\infty(w) = C\psi_2^\infty(C'w) \end{cases} \tag{1.15}$$

The analytic part of the modulus is given by the equivalence class $[\psi^0, \psi^\infty]$.

- The formal part a can be recovered from the analytic part since $(\psi^0)'(0)(\psi^\infty)'(0) = \exp(2\pi i a)$. So the Ecalle-Voronin modulus is $(k = 1, [\psi^0, \psi^\infty])$.

To interpret the analytic part of the modulus we must describe the "normal form" of f_0, which we call the *model diffeomorphism*. It is given by the time-one map of the flow of the vector field

$$\frac{z^2}{1+az}\,\frac{\partial}{\partial z}. \tag{1.16}$$

There always exist a change of coordinate conjugating f_0 to the model diffeomorphism. The formal change of coordinate can be summed to an analytic one if and only if ψ^0 and ψ^∞ are linear. The reason why the time-one map of the flow of (1.16) is a model is because

this diffeomorphism is "fully iterable": we can take its n-root for any n and, more generally, define $f^{\circ c}$, where c is a complex number.

An interpretation of the analytic part of the modulus: The nonlinearities of ψ^0 and ψ^∞ control *parametric resurgence phenomena* in the unfolding (1.13). Then

- ψ^0 (resp. ψ^∞) controls $-\sqrt{\epsilon}$ (resp. $\sqrt{\epsilon}$) when its multiplier is on the unit circle.
- If
$$\psi^\infty(w) = w + \sum_{n=2}^{\infty} b_n w_n \tag{1.17}$$
then $\forall p, q, \in N$ with $1 \leq q < p$ there exists polynomials
$$L^\infty_{p,q}(b_2, \ldots, b_{p+1}) \tag{1.18}$$
such that if $L^\infty_{p,q}(b_2, \ldots, b_{p+1}), \neq 0$ then f_ϵ is non linearizable at $\sqrt{\epsilon}$ as soon as the multiplier $\lambda = f'_\epsilon(\sqrt{\epsilon})$ is of the form
$$\lambda = \exp(2\pi i \frac{p}{n}) \tag{1.19}$$
with n large and
$$n \equiv q \ (\mathrm{mod}\ p). \tag{1.20}$$
- If ψ^∞ is nonlinear, then at least one of the $L^\infty_{p,q}(b_2, \ldots, b_{p+1}) \neq 0$.
- A similar result exists with ψ^0 controlling $-\sqrt{\epsilon}$. If $a \neq 0$ we cannot simultaneously scale $\psi^{\infty\prime}(0) = 1$ and $\psi^{0\prime}(0) = 1$.

1.2 An answer to a question of Martinet-Ramis

In [32] Martinet-Ramis study the modulus of a saddle-node. They show that the analytic type of a saddle-node is characterized by the analytic type of the holonomy of the strong separatrix, which is a diffeomorphism with a parabolic fixed point. However not all diffeomorphisms with a parabolic fixed point can be realized as the holonomy map of the strong separatrix of a saddle-node, yielding that the moduli space of the holonomy maps of strong separatrices of saddle-nodes is strictly smaller that the moduli space of diffeomorphims with a parabolic fixed point. Martinet and Ramis ask the following question: (the equation (2) to which they refer is our equation (1.5)): *"Un phénomène qui reste un peu surprenant à nos yeux est que les holonomies produites par les équations (2) ne sont pas arbitraires: on obtient seulement une "petite partie du module d'Ecalle". (Nous nous proposons de montrer dans un article ultérieur qu'il n'en est plus de même dans le cas des équations résonantes "non dégénérées" ($\lambda = -p/q \neq 0$): le module des classes d'équivalence analytiques d'équations différentielles s'identifie complètement au "module d'Ecalle")."*. Indeed the modulus of the holonomy of the strong separatrix of a saddle-node has the form $([\psi^0, \psi^\infty])$ where
$$\psi^\infty(w) = \frac{w}{1 - bw}. \tag{1.21}$$

The answer comes from the following theorem:

1.1 Theorem *[33] The only analytic function $\psi^\infty(w)$ of the form* (1.17) *for which*

$$\forall p > 1, \forall q \quad L^\infty_{p,q}(b_2, \ldots, b_{p+1}) = 0 \tag{1.22}$$

is the Möbius function (1.21)*.*

Hence the Möbius function is the only function which can reflect the very simple dynamics of the node in the unfolding. Any other function would force the node to have a more complex dynamics, in particular to be nonlinearizable for non resonant cases.

2 Modulus of analytic classification of generic families unfolding a diffeomorphism with a generic parabolic point

We now present the results of [33]. We consider a generic diffeomorphism $f_0(z)$ with a parabolic fixed point as in (1.14). An unfolding is *generic* if

$$\left.\frac{\partial f_\epsilon}{\partial \epsilon}\right|_{\epsilon=0} \neq 0. \tag{2.1}$$

We classify germs of analytic families of diffeomorphims under *weak equivalence.*

2.1 Preliminaries

2.1 Definition Two germs $f_{1,\epsilon_1}(z)$ and $f_{2,\epsilon_2}(z)$ of analytic families of diffeomorphims are *weakly equivalent* if there exists a germ of bijective map $K = (h, H)$:

$$(\epsilon_1, z) \mapsto (h(\epsilon_1), H(\epsilon_1, z)) \tag{2.2}$$

fibered over the parameter space where:

i) h is a germ of holomorphic diffeomorphism $(C, 0) \to (C, 0)$.

ii) there exists a representative $H(\epsilon_1, z)$ for $(z, \epsilon_1) \in U \times V$ such that

- $H_{\epsilon_1} = H(\epsilon_1, .)$ is analytic in z for $z \in U$;
- H_{ϵ_1} conjugates f_{1,ϵ_1} and $f_{2,h(\epsilon_1)}$ over U, for all $\epsilon_1 \in V$, namely:

$$f_{2,h(\epsilon_1)}(H_{\epsilon_1}(z)) = H_{\epsilon_1}(f_{1,\epsilon_1}(z)). \tag{2.3}$$

We will show that if two generic families unfolding a diffeomorphism with a generic parabolic point are weakly equivalent, then they are equivalent in a stronger sense.

"Preparation" of an unfolding $f_\epsilon(z)$ of $f_0(z)$.

We can suppose that the two singular points are located at $\pm\sqrt{\epsilon}$, i.e. $f_\epsilon(z)$ has the form (1.13). We want to compare our family with the "model family" which is given by the time-one map of the flow of the vector field

$$\frac{z^2-\epsilon}{1+a(\epsilon)z}\,\frac{\partial}{\partial z}. \tag{2.4}$$

(From now on we will not write the dependence of $a(\epsilon)$ and simply denote $a=a(\epsilon)$.) The singular points of (2.4) are $\pm\sqrt{\epsilon}$. Their eigenvalues are

$$\mu_\pm = \pm\frac{2\sqrt{\epsilon}}{1\pm a\sqrt{\epsilon}} \tag{2.5}$$

and satisfy

$$\begin{array}{rcl} \frac{1}{\sqrt{\epsilon}} & = & \frac{1}{\mu_+}-\frac{1}{\mu_-} \\ a & = & \frac{1}{\mu_+}+\frac{1}{\mu_-}, \end{array} \tag{2.6}$$

i.e. in the model family a and ϵ are analytic invariants.

We make a change of coordinate $(z,\epsilon)\mapsto(\overline{z},\overline{\epsilon})$ in $f_\epsilon(z)$:

$$\overline{f}_{\overline{\epsilon}}(\overline{z}) = \overline{z}+(\overline{z}^2-\epsilon)\overline{h}(\overline{z},\overline{\epsilon}), \tag{2.7}$$

so that $\overline{\epsilon}$ becomes an analytic invariant, i.e.

$$\frac{1}{\sqrt{\overline{\epsilon}}} = \frac{1}{\ln\lambda_+}-\frac{1}{\ln\lambda_-}, \tag{2.8}$$

where $\lambda_\pm$ are the multipliers at the singular points $\pm\sqrt{\overline{\epsilon}}$ of (2.4), (in which we replace (z,ϵ) by $(\overline{z},\overline{\epsilon})$). Then for the model family (2.4) we choose

$$a(\epsilon) = \frac{1}{\ln\lambda_+}+\frac{1}{\ln\lambda_-}. \tag{2.9}$$

The new family $\overline{f}_{\overline{\epsilon}}(\overline{z})$ is called "prepared". $\overline{\epsilon}$ is the canonical parameter of the family.

From now on we will limit ourselves to prepared families (1.13). Because the parameter is an analytic invariant then **weak equivalence between prepared families must preserve the parameter.**

Here are some general principles to guide us in the definition of a complete modulus of analytic classification for prepared families:

- We must cover a whole neighborhood of the origin in parameter space.
- We try to have as much continuity and smoothness in ϵ as possible.
- But it may be difficult to make a full turn in ϵ, so it is natural to work with the universal covering of the ϵ-space.

2.2 Description of the modulus of analytic classification for the family

i) We give ourselves $\delta > 0$ arbitrarily small.

We consider the universal covering of the ϵ-space and call $\hat{\epsilon}$ the corresponding variable and we have the projection $\pi(\hat{\epsilon}) = \epsilon$.

ii) We describe the orbit space of a prepared family (1.13) for all neighborhoods $\{z; |z| < r\}$ with $r \leq r_0$, where r_0 depends on δ, for all values of $\hat{\epsilon}$ such that

$$\begin{cases} |\hat{\epsilon}| < \rho < Kr \\ \arg \hat{\epsilon} \in (-\pi + \delta, 3\pi - \delta) \end{cases} \tag{2.10}$$

(Figure 7), where $K > 0$ is a positive constant depending on r_0 and δ. This neighborhood covers only once the Siegel direction R^-. We call V_δ this sector.

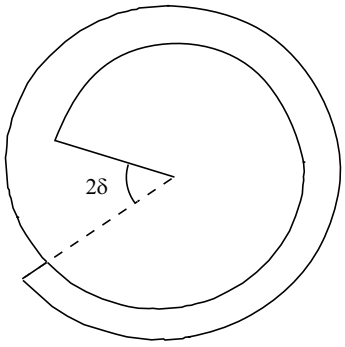

Figure 7: The sector V_δ in $\hat{\epsilon}$-space

A similar description can be done in a second sector

$$\begin{cases} |\hat{\epsilon}| < \rho < Kr \\ \arg \hat{\epsilon} \in (-3\pi + \delta, \pi - \delta). \end{cases} \tag{2.11}$$

The union of the two neighborhoods covers a full neighborhood of 0 in the $\sqrt{\epsilon}$-space.

iii) $\forall \hat{\epsilon} \in V_\delta$ the orbit space is described by two crescents $C^\pm_\epsilon$, which:

- are fundamental domains for f_ϵ;
- whose quotient by f_ϵ have the conformal structure of spheres $S^\pm_\epsilon$, the points $\sqrt{\epsilon}$ (resp. $-\sqrt{\epsilon}$) corresponding to ∞ (resp. 0);
- in the two ends of the crescents, (i.e. near 0 and ∞ on the spheres $S^\pm_\epsilon$) points are identified by germs of analytic diffeomorphisms ψ^∞_ϵ and ψ^0_ϵ (Figure 8).

iv) It is possible to choose the $C^\pm_\epsilon$ depending analytically on $\hat{\epsilon}$ for $\hat{\epsilon} \neq 0$ and continuously on $\hat{\epsilon}$ near $\hat{\epsilon} = 0$.

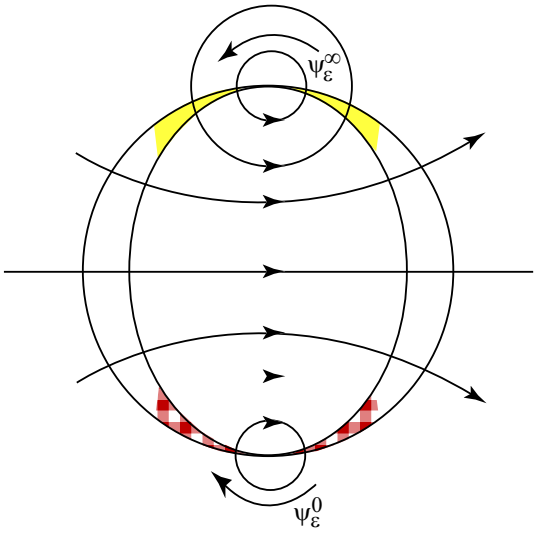

Figure 8: The two crescents and diffeomorphisms ψ_ϵ^∞ and ψ_ϵ^0

v) The cordinates on the spheres can be chosen so that the functions ψ_ϵ^∞ and ψ_ϵ^0 depend analytically on $\hat{\epsilon}$ for $\hat{\epsilon} \neq 0$ and continuously on $\hat{\epsilon}$ near $\hat{\epsilon} = 0$.

vi) We define the usual equivalence relation

$$(\psi_{1,\epsilon}^0, \psi_{1,\epsilon}^\infty) \equiv (\psi_{2,\epsilon}^0, \psi_{2,\epsilon}^\infty) \quad \text{iff} \quad \exists C, C' \in C^* \begin{cases} \psi_{1,\epsilon}^0(w) = C\psi_{2,\epsilon}^0(C'w) \\ \psi_{1,\epsilon}^\infty(w) = C\psi_{2,\epsilon}^\infty(C'w) \end{cases} \tag{2.12}$$

vii) $\forall \hat{\epsilon} \in V_\delta$ $[(\psi_\epsilon^0, \psi_\epsilon^\infty)]$ is a complete modulus of analytic classification for f_ϵ.

2.2 Theorem *[33] The family* $\{[(\psi_{\hat{\epsilon}}^0, \psi_{\hat{\epsilon}}^\infty)]\}|_{\hat{\epsilon} \in V_\delta}$ *is a complete modulus of analytic classification of the family* $\{f_\epsilon\}$.

Proof We just give an idea of the proof: it is a generalization of ideas of Lavaurs and Shishikura (their method applies to smaller sectors in ϵ-space as in Figure 9).

It uses the construction of Fatou coordinates embedding f_ϵ into the time-one map of (2.4) by means of the Ahlfors-Bers theorem [25].

- We lift f_ϵ by means of

$$Z = \begin{cases} \frac{1}{2\sqrt{\epsilon}} \ln \frac{z-\sqrt{\epsilon}}{z+\sqrt{\epsilon}} & \epsilon \neq 0 \\ -\frac{1}{z} & \epsilon = 0. \end{cases} \tag{2.13}$$

  The image of $U \setminus \{\pm\sqrt{\epsilon}\}$ is $\hat{U}$, which is $C \setminus B_0$ (resp. $C \setminus \cup_{k \in Z} B_k$) where the B_k are disjoint simply connected domains of C. B_0 contains the origin and is called the *fundamental hole*.

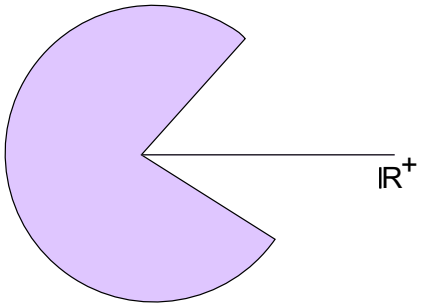

Figure 9: Type of sectors in ϵ-space in Shishikura's paper

- This change of coordinates has the property of transforming the diffeomophism f_ϵ to a small perturbation of the translation by 1. Namely $f_\epsilon(z)$ becomes

$$F_\epsilon(Z) = Z + 1 + R(\epsilon, Z), \tag{2.14}$$

with $R(\epsilon, Z)$ and $\frac{\partial}{\partial Z} R(\epsilon, Z)$ small.

- We consider *admissible lines* l, which are lines such that ℓ and $F_\epsilon(\ell)$ generate fundamental domains $\hat{C}_\epsilon$ for F_ϵ (Figure 10).

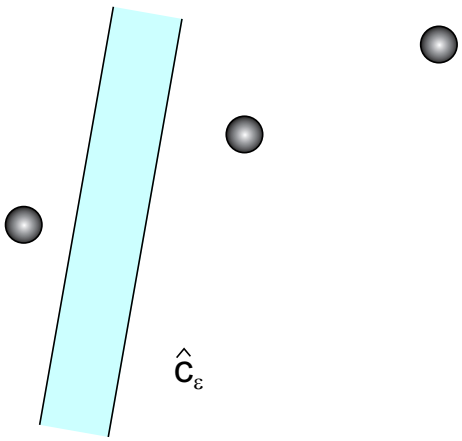

Figure 10: A fundamental domain generated by an admissible line

- Families of admissible lines can be chosen depending continuously on $\hat{\epsilon} \in V_\delta$ (and analytically of $\hat{\epsilon} \neq 0$) as in Figure 11.

- The admissible lines generate *translation domains* $Q(\ell)$:

$$Q(\ell) = \{Z | \exists n \in Z,\ F_\epsilon^n(Z) \in \hat{C}_\epsilon \text{ and } \forall m \in [0, n] F_\epsilon^m \in \hat{U}\}. \tag{2.15}$$

Remark that a translation domain is independent of the admissible line which generates it, as long as the admissible line is deformed within $\hat{U}$ while remaining admissible.

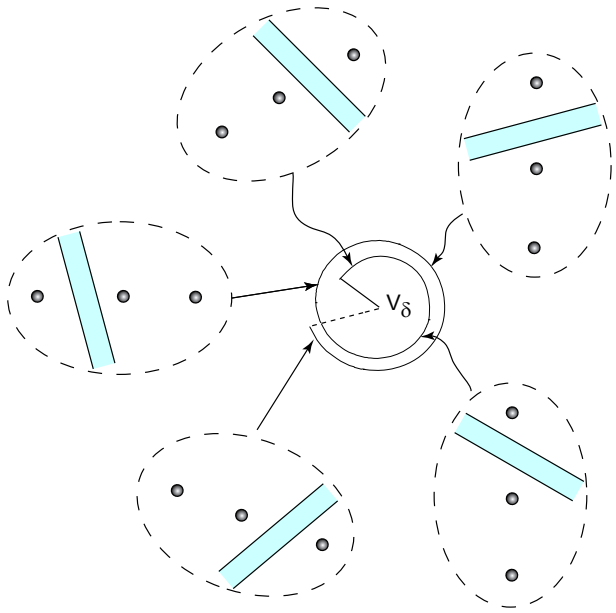

Figure 11: Admissible lines depending continuously on $\hat{\epsilon}$

- On a translation domain Q we construct a Fatou coordinate Ψ_ϵ conjugating F_ϵ with $Z \mapsto Z+1$:

$$\Phi_\epsilon(F_\epsilon(Z)) = \Phi_\epsilon(Z) + 1. \tag{2.16}$$

Fatou coordinates are holomorphic diffeomorphisms. Moreover they are uniquely defined up to a translation.

The construction is done in two steps

i) We first construct in a very rough way a homeomorphism $h : Q \to C$ conjugating F_ϵ with $Z \mapsto Z+1$. If $\ell = \{Z_1 + Ye^{i\theta} | Y \in R\}$, then

$$h^{-1}(X,Y) = (1-X)(Z_1 + Ye^{i\theta}) + XF_\epsilon(Z_1 + Ye^{i\theta}). \tag{2.17}$$

ii) The mapping h^{-1} is quasi-conformal. Indeed let

$$\mu = \frac{\partial h^{-1}/\partial \overline{Z}}{\partial h^{-1}/\partial Z}. \tag{2.18}$$

We extend μ in a periodic way to all of C by the translation $Z \mapsto Z+1$. The map μ is in $L^\infty(C)$ and has L^∞-norm $||\mu||_\infty < 1$. So μ is a Beltrami field. It induces $\tilde{\mu}$ on S^2 by means of $Z \mapsto \exp(-2\pi i Z)$ and we let $\tilde{\mu}(0) = \tilde{\mu}(\infty) = 0$.

By Ahlfors-Bers measurable mapping theorem, if μ_0 is the standard conformal structure on S^2, then

$$\exists! \tilde{h}_1 : S^2 \to S^2 \tag{2.19}$$

such that

$$\begin{cases} \tilde{h}_1^* \mu_0 = \tilde{\mu} \\ \tilde{h}_1(0) = 0 \\ \tilde{h}_1(\infty) = \infty \\ \tilde{h}_1(1) = 1. \end{cases} \tag{2.20}$$

We lift $\tilde{h}_1$ to h_1 such that $h_1(0) = 0$ and $h_1(1) = 1$. Then

$$\Phi = h_1 \circ h \tag{2.21}$$

is quasi-conformal and preserves the standard conformal structure. Hence Φ is conformal and conjugates f_ϵ with $Z \mapsto Z + 1$.

- If we choose a base point $Z_0(\epsilon)$ depending holomorphically on ϵ, then the unique Fatou coordinate satisfying $\Phi_\epsilon(Z_0(\epsilon)) = 0$ depends continuously on $\hat{\epsilon}$ near $\hat{\epsilon} = 0$ and holomorphically on $\hat{\epsilon} \neq 0$.

□

There exists two different ways of constructing the modulus:

I. We take two Fatou coordinates $\Phi_\epsilon^\pm$ associated to two admissible lines passing between holes and located on the two sides of the fundamental hole (Figure 12).

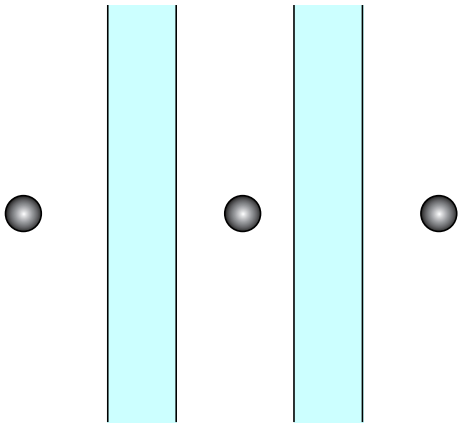

Figure 12: Two fundamental domains on each side of the fundamental hole

The modulus is defined as

$$\Psi_\epsilon = \Phi_\epsilon^+ \circ (\Phi_\epsilon^-)^{-1}. \tag{2.22}$$

It is defined on a domain as in Figure 13.

Using $Z \mapsto \exp(-2\pi i Z)$ this yields the two diffeomorphisms ψ_ϵ^∞ and ψ_ϵ^0 of Figure 8, which are the unfolding of the Ecalle-Voronin modulus.

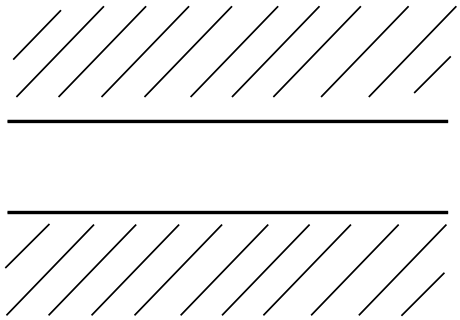

Figure 13: The domain of the modulus Ψ_ϵ

II. The second method does not pass to the limit when $\epsilon \to 0$ but it allows to study the dynamics of $\sqrt{\epsilon}$. Indeed we have a global transition diffeomorphism, called the *Lavaurs map*

$$L_\epsilon : S_\epsilon^- \to S_\epsilon^+ \tag{2.23}$$

sending a point $w \in S_\epsilon^-$ to the first point of S_ϵ^+ belonging to the orbit of w under f_ϵ when iterating f_ϵ positively. As the Lavaurs map is global and sends 0 to) and ∞ to ∞ it is linear:

$$w \mapsto L_\epsilon(w) = \tau(\epsilon)w \tag{2.24}$$

with $\tau(\epsilon) \neq 0$. This second point of view allows to define *renormalized return maps* and to describe the *parametric resurgence*.

The renormalized return maps. They are defined as $k_\epsilon^\infty, k_\epsilon^0 : S_\epsilon^+ \to S_\epsilon^+$ (Figure 14) as:

$$\begin{array}{rcl} k_\epsilon^\infty(w) & = & \tau(\epsilon)\psi_\epsilon^\infty(w) \\ k_\epsilon^0(w) & = & \tau(\epsilon)\psi_\epsilon^0(w). \end{array} \tag{2.25}$$

The derivatives of k_ϵ^∞ at ∞ (resp. k_ϵ^0 at 0) are analytic invariants:

$$\begin{array}{rcl} k_\epsilon^{0\prime}(0) & = & \exp(4\pi^2/\mu_-) \\ k_\epsilon^{\infty\prime}(\infty) & = & \exp(4\pi^2/\mu_+). \end{array} \tag{2.26}$$

(Note that ∞ (resp. 0) corresponds to $\sqrt{\epsilon}$ (resp. $-\sqrt{\epsilon}$)).

The parametric resurgence.

We will limit ourselves to describe the parametric resurgence at $-\sqrt{\epsilon}$ by means for ψ_ϵ^0. Let us first remark that it is possible to choose coordinates on S_ϵ^+ and S_ϵ^- so that

$$\psi_\epsilon^0(w) = w + \sum_{n>1} b_n(\epsilon) w^n, \tag{2.27}$$

with the $b_n(\epsilon)$ depending continuously on ϵ. In particular for $\epsilon = 0$

$$\psi^0(w) = w + \sum_{n>1} b_n w^n, \tag{2.28}$$

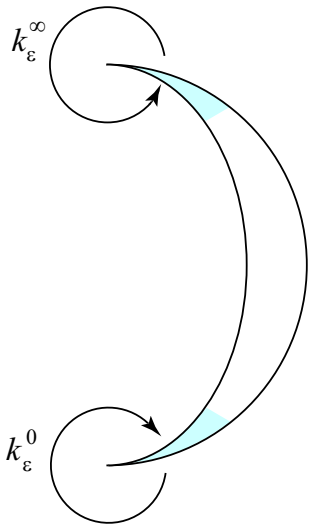

Figure 14: The return maps on S_ϵ^+

where $b_n = b_n(0)$, is half of the Ecalle-Voronin modulus . Hence if ψ^0 is nonlinear, then ψ_ϵ^0 is nonlinear for all small ϵ.

The particular case where $\mu_- = \exp\left(-\frac{2\pi i}{n}\right)$, with n large. Then

$$k_\epsilon^{0\prime}(0) = 1. \tag{2.29}$$

Hence k_ϵ^0 nonlinear implies that k_ϵ^0 non linearizable.

The general case. We consider the resonances

$$\mu_- = \exp\left(-\frac{2\pi i p}{n}\right), \qquad n \equiv q \ (\mathrm{mod}\ p) \tag{2.30}$$

with n large. Then

$$k_\epsilon^{0\prime}(0) = \exp\left(2\pi i \frac{q}{p}\right). \tag{2.31}$$

2.3 Theorem *[33] If*

$$g(w) = \exp\left(2\pi i \frac{q}{p}\right) \psi^0(w) \tag{2.32}$$

is nonlinearizable, then k_ϵ^0 is non linearizable for ϵ such that

$$\begin{cases} \mu_- = \exp\left(-2\pi i \frac{p}{n}\right) \\ n \ large \\ n \equiv q \ (mod\, p). \end{cases} \tag{2.33}$$

This occurs as soon as one of the coefficients of the normal form of $g(w)$ does not vanish. The k-th coefficient of the normal form of $g(w)$ is a quasi-homogeneous polynomial

$$L^k_{p,q}(b_2, \dots b_{kq+1}). \tag{2.34}$$

2.3 The two ways to normalize to the model

The Fatou coordinates allow us to find a normalizing transformation to the model.

We have embedded the diffeomorphism into the model in the middle (between $\pm\sqrt{\epsilon}$) and read the incompatibility when turning around $\pm\sqrt{\epsilon}$: we have found a change of coordinate transforming $f_\epsilon(z)$ to the model over a ramified neighborhood of $\pm\sqrt{\epsilon}$ for $\hat{\epsilon} \in V_\delta$ (Figure 15).

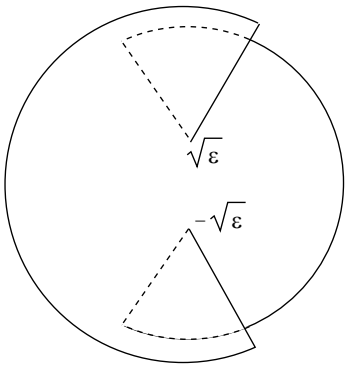

Figure 15: The domain on which the diffeomorphism is embedded in the model

We compare this point of view with the Glutsyuk point of view [15] which was already introduced by Martinet [26].

Glutsyuk works for values of ϵ in a sector V

$$\begin{cases} |\epsilon| < r \\ \arg(\epsilon) \in (-\pi + \delta, \pi - \delta). \end{cases} \tag{2.35}$$

For any such $\epsilon \in V$, the diffeomorphism f_ϵ is linearizable in the neighborhood of $\pm\sqrt{\epsilon}$. Glutsyuk finds two changes of coordinates defined in neighborhoods of each singular point transforming $f_\epsilon(z)$ to the linear model in the neighborhood of $\pm\sqrt{\epsilon}$. He reads the incompatibility on the intersection of the two neighborhoods (Figure 16).

Our method allows to recover Glutsyuk results. Indeed it suffices to take two admissible lines parallel to the lines of holes and located on each side of the line of holes (Figure 17).

They generate translation domains Q^0 and Q^∞ on which we have Fatou coordinates Φ^0_ϵ and Φ^∞_ϵ. Φ^0_ϵ and Φ^∞_ϵ are changes of coordinates transforming the diffeomorphism to the model diffeormorphism. As the model is linearizable near $\pm\sqrt{\epsilon}$ this is equivalent to find linearizing changes of coordinates. The *Glutsyuk modulus* is then given by

$$\Psi^G_\epsilon = \Phi^0_\epsilon \circ (\Psi^\infty_\epsilon)^{-1}. \tag{2.36}$$

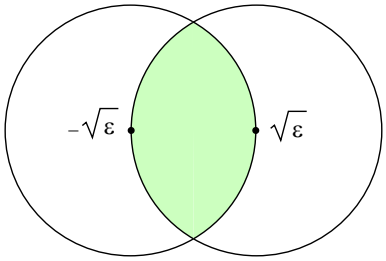

Figure 16: The fundamental domains in Glutsyuk point of view

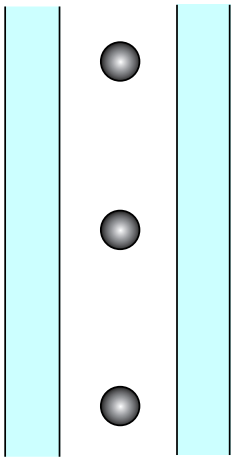

Figure 17: The admissible lines in Glutsyuk point of view

The Glutsyuk modulus is equivalent to the modulus $[(\psi_\epsilon^0, \psi_\epsilon^\infty)]$ described before (see [33]).

In the Glutsyuk point of view we normalize near the singular points $\pm\sqrt{\epsilon}$ and read the incompatibility in the middle.

3 Applications

One motivation for the previous study comes from work of the author with P. Mardešić and C. Christopher, [5] and [4]. In these papers we tried to understand how the strata of integrable and linearizable systems at the origin are organized in a family of polynomial systems

$$\begin{array}{rcl} \dot{x} & = & x + \sum_{i+j=2}^{n} a_{ij} x^i y^j \\ \dot{y} & = & -\lambda y + \sum_{i+j=2}^{n} b_{ij} x^i y^j \end{array} \tag{3.1}$$

where $\lambda \in R^+$ and $a_{ij}, b_{ij} \in C$. We observed strange behaviours which we can now explain with the new tools developed in the previous section.

In [4] we study the family of Lotka-Volterra systems:

$$\begin{array}{rcl} \dot{x} & = & x(1 + ax + by) \\ \dot{y} & = & y(-\lambda + cx + dy) \end{array} \tag{3.2}$$

where we want to identify all integrable systems for all $\lambda = \frac{p}{q} \in Q^+$. A characterization exists for all $\lambda \in N \cup 1/N$ ([14] and [17]). Also all Darboux integrable systems are known [3]. As the system is simple we could calculate saddle quantities for several values of $\lambda \in Q^+$ and come with the following conjecture:

3.1 Conjecture [4] Two mechanisms are sufficient to describe all systems (3.2) with an integrable point at the origin:

i) The system has one extra invariant algebraic curve apart from the two axes. (Limit cases are possible when one of the axes or the equator is a multiple invariant algebraic curve).

ii) The system is invariant by the "monodromy argument".

The monodromy argument. This argument deals with the monodromy group of one of the two axes which are the separatrices of the origin. Let us describe it on the x-axis. The system has three singular points on $x = 0$, namely $(0, 0)$, $P_1 = (-1/a, 0)$ and P_∞ which is the point at infinity.

- It is known that the origin is integrable if and only if its monodromy map M_0 is linearizable.
- M_0 is conjugate to $M_\infty^{-1} \circ M_1^{-1}$ where M_1 (resp. M_∞) is the monodromy of P_1 (resp. P_∞), see Figure 18.

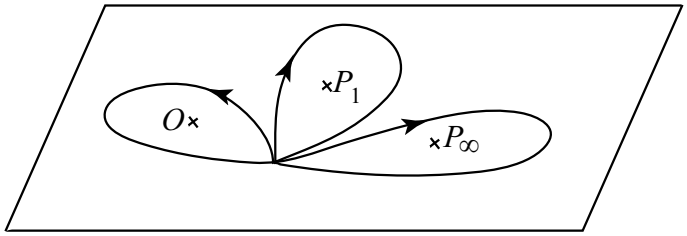

Figure 18: The monodromy group of the x-separatrix

- Hence a first sufficient condition for the linearizability of M_0 is given by $M_\infty \equiv id$ and M_1 linearizable. $M_\infty \equiv id$ as soon as it is a resonant node with eigenvalues μ_1, μ_2 with $\mu_2/\mu_1 \in N$ (we have no problem of resonance as the node has two analytic separatrices). Moreover M_1 is linearizable as soon as it is a non resonant node or a resonant node with a zero resonant monomial.
- Similarly a second sufficient condition for the linearizability of M_0 is given by $M_1 \equiv id$ and M_∞ linearizable. This is realized if the eigenvalues ν_1, ν_2 of P_1 satisfy $\nu_2/\nu_1 \in N$ and M_∞ linearizable. To realize M_∞ linearizable we have two choices: either P_∞ is a node (we have no problem of resonance as the node has two analytic separatrices) or it is a saddle and we play the monodromy argument on the line at infinity.

3.2 Theorem *[4] These two mechanisms are sufficient to provide necessary and sufficient conditions for integrability in the Lotka-Volterra system* (3.2) *for the following rational values of* λ*:*

- $\lambda = n, 1/n$. *This case was already studied in [14] but other arguments were used to prove that the conditions were necessary and sufficient.*
- $\lambda = n/2, 2/n$. *This case was already studied in [17] but other arguments were used to prove that the conditions were necessary and sufficient.*
- $\lambda = \frac{p}{q}$, $p + q \leq 12$.

The paper [4] also lists general conditions of integrability. One is the following:

Condition (*).
The system (3.2) is integrable if

$$(*) \begin{cases} a = -c \\ \lambda > 1,\ \lambda \neq 1 + \frac{1}{m} \text{ with } m \in N. \end{cases} \tag{3.3}$$

If $\lambda = 1 + \frac{1}{m}$, an additional condition is necessary for integrability.

Let us explain condition (*). The condition $a = -c$ guarantees that P_∞ is a node with eigenvalues in the ratio $1 : 2$ yielding $M_\infty \equiv id$. The condition $\lambda > 1$ guarantees that P_1 is a node. If $\lambda \neq 1 + \frac{1}{m}$ the node is non resonant, yielding that M_1 is linearizable. If $\lambda = 1 + \frac{1}{m}$ then the node is resonant with eigenvalues in the ratio $n : 1$ and we need to ask that the resonant monomial has a zero coefficient.

In practice when $b, c \neq 0$ we can scale $b = c = 1$ yielding $a = -1$ and the family depends only on the parameter d:

$$\begin{aligned} \dot{x} &= x(1 - x + y) \\ \dot{y} &= x(-\lambda + x + dy). \end{aligned} \tag{3.4}$$

Then condition (*) yields a stratum of dimension 1 (resp. strata of dimension 0) when $\lambda > 1$, $\lambda \neq 1 + 1/m$ (resp. $\lambda = 1 + 1/m$), see Figure 19. The pathological values $\lambda = 1 + 1/m$ accumulate to $\lambda = 1$. So the following questions are natural:

Questions:

(1) What happens for $\lambda = 1$? Indeed the integrable points for $\lambda = 1 + 1/m$ of Figure 19 show a nice pattern of sequences with accumulation points on $\lambda = 1$.

(2) What happens for $\lambda < 1$?

Computational answers:

(1) Calculations yield that for $\lambda = 1$ the origin is integrable only if $d = -1$. So all limit points except one are not integrable.

(2) Calculations on the side $\lambda < 1$, in particular for $\lambda = 1 - 1/m$ show that points seem generically non integrable, so the pattern seems not to be symmetric.

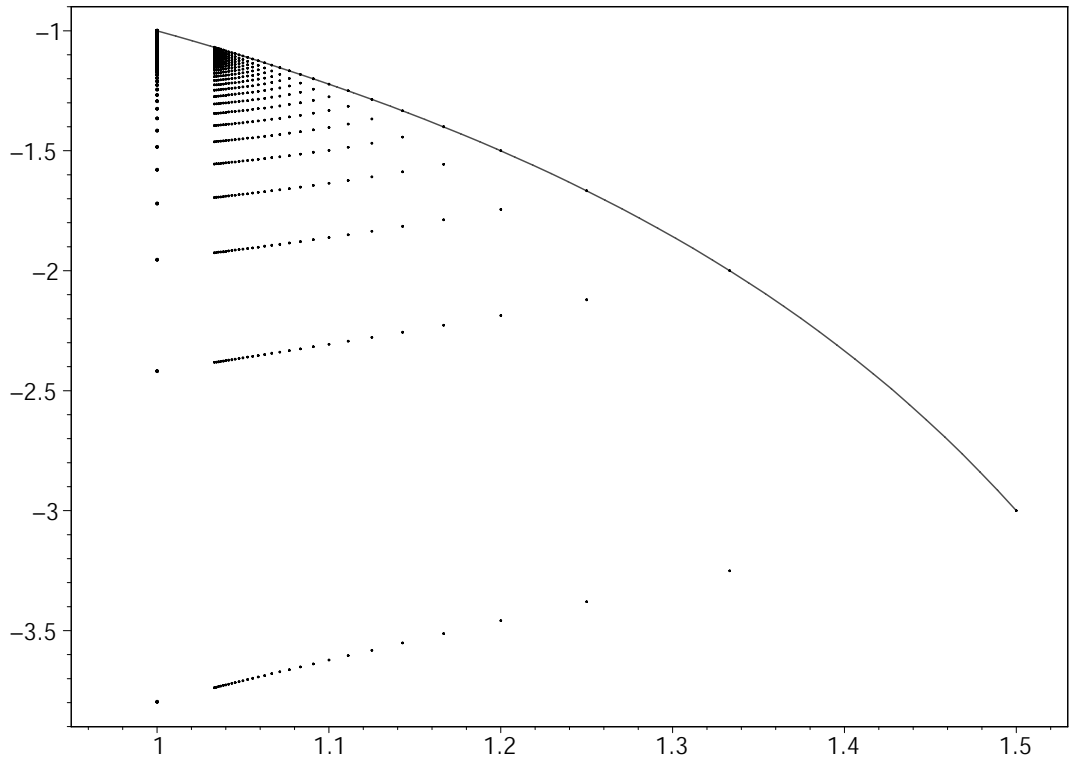

Figure 19: The values of d for which the system (3.4) is integrable for $\lambda = 1 + 1/n$. The system is integrable on the curve $d = \frac{\lambda}{\lambda - 2}$.

Explanation: Except for $d = -1$ the map M_0 has a generic parabolic point as studied in the previous section. The limit points at $\lambda = 1$ in Figure 19 are *semi-normalizable*: If (ψ^0, ψ^∞) is the Ecalle-Voronin modulus of M_0, then we have

$$\begin{cases} \psi^\infty \text{ linear} \\ \psi^0 \text{ non linear.} \end{cases} \tag{3.5}$$

At $\lambda = 1$ we have a *transcritical bifurcation*. Indeed M_0 has two fixed points for $\lambda \neq 1$ and a double fixed point for $\lambda = 1$. The first fixed point is the origin and the second fixed point corresponds to an invariant manifold [22]. These two points "pass through each other" at $\lambda = 1$ as is usual in a transcritical bifurcation (Figure 20):

- For $\lambda < 1$, ψ^∞ controls the invariant manifold while ψ^0 controls the origin. Hence the origin is necessarily non trivial by Theorem 2.3 for $\lambda = 1 - 1/m$ with m large, while the invariant manifold may or may not be trivial.
- For $\lambda > 1$, ψ^∞ controls the origin which can hence be integrable if $d(\lambda)$ is well chosen, while ψ^0 controls the invariant manifold which is necessarily nontrivial for $\lambda = 1 + 1/m$ by Theorem 2.3.

Other consequence: For $\lambda = 1$ we can say more about the points which are not limit points of sequences of integrable systems for $\lambda = 1 + 1/m$. These points are approached by

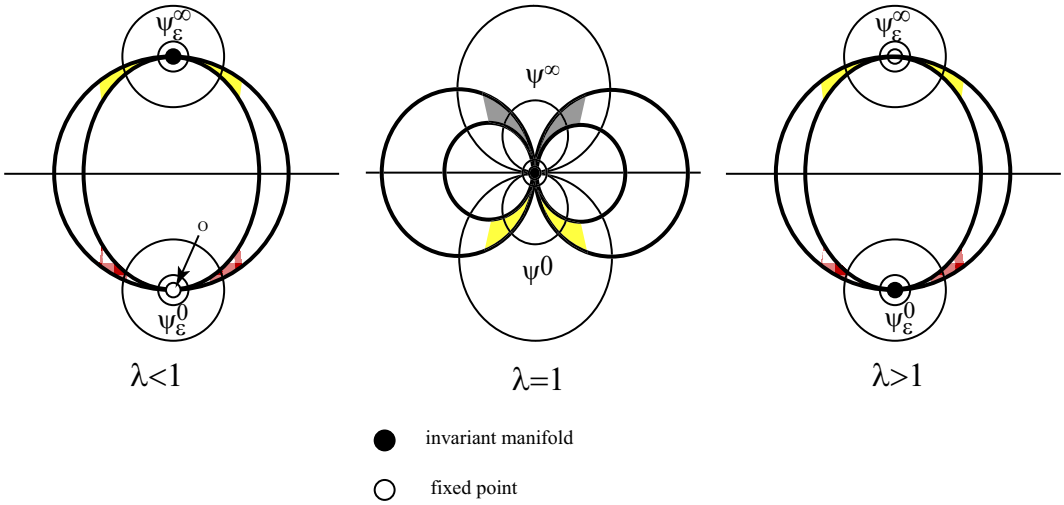

Figure 20: The transcritical bifurcation

integrable saddles as soon as $\lambda \neq 1 + 1/m$. If (ψ^0, ψ^∞) is the Ecalle-Voronin modulus of the limit point, then we know that the unfolding ψ^∞ controls the origin for $\lambda > 1$. Hence necessarily ψ^∞ is a Möbius function by Theorem 1.1.

4 The finiteness part of Hilbert's 16th problem for quadratic systems

Hilbert's 16th problem asks for the maximum number $H(n)$ of limit cycles of a polynomial planar vector field of degree $\leq n$. It is still open for any n. Since the simultaneous proofs of Ecalle and Ilyashenko in 1987 it is known that a single vector field has a fnite number of limit cycles. The finiteness part of Hilbert's 16th problem deals with the existence of a uniform bound for the number of limit cycles of a polynomial system of degree $\leq n$:

The finiteness part of Hilbert's problem for polynomial vector fields. $\forall n \in N \; \exists M(n) \in N$ such that any polynomial vector field

$$\begin{array}{rcl} \dot{x} & = & P(x,y) \\ \dot{y} & = & Q(x,y) \end{array} \tag{4.1}$$

with $P, Q, \in R[x,y]$ and $\max(\deg(P), \deg(Q)) \leq n$ has at most $M(n)$ limit cycles. It is usually given in the condensed form

$$H(n) < \infty. \tag{4.2}$$

In [9] a strategy was developed to attack the finiteness part in the particular case $n = 2$. The idea of the strategy is the following. It is possible to compactify the phase space to the Poincaré sphere. Hence, if there is an infinite number of limit cycles then they need to accumulate on some graphics. This idea is sufficient to prove that any individual polynomial vector field has a finite number of limit cycles. For quadratic systems the proof is elementary

[2]. Moreover the coefficients of the system are parameters. Rescaling time it is possible to consider the parameter space of nonzero vector fields of degree ≤ 2 as a compact space. Limit cycles depend on the parameters and accumulate on "limit periodic sets", which we want to look at as "local" objects. If all these limit periodic sets have *finite cyclicity*, a "local finiteness property", then we can expect a uniform bound for the number of limit cycles.

Notation for the figures: In all this section double arrows on an invariant manifold in the figures indicate hyperbolicity in that direction, i.e. the corresponding eigenvalue is nonzero.

4.1 Definition A limit periodic set Γ of a vector field v_{λ_0} has *finite cyclicity inside a family of vector fields* $\{v_\lambda\}_{\lambda\in\Lambda}$ if $\exists\epsilon > 0, \delta > 0$, $\exists N \in N$ such that any v_λ with $|\lambda - \lambda_0| < \delta$ has at most N limit cycles $\gamma_1, \ldots \gamma_m$ such that $d_H(\gamma_i, \Gamma) < \epsilon$, where d_H is the Hausdorff distance between compact sets.

4.2 Theorem *[9]*

$$H(2) < \infty. \tag{4.3}$$

if and only if all 121 limit periodic sets surrounding the origin in the family

$$\begin{aligned} \dot{x} &= \lambda x - \mu y + a_1 x^2 + a_2 xy + a_3 y^2 \\ \dot{y} &= \mu x + \lambda y + b_1 x^2 + b_2 xy + b_3 y^2, \end{aligned} \tag{4.4}$$

$(\lambda, \mu) \in S^1$, $(a_1, a_2, a_3, b_1, b_2, b_3) \in S^5$ *have finite cyclicity inside the family* (4.4).

Although the paper [9] was published in 1994, the program is started since 1991. It progresses well. The purpose of the present section is to present its actual status with a discussion on what is done and what remains to be done. Since 1994 no error was found in the list of graphics of [9]. The author however feels that the list should have contained 125 graphics. Indeed the list of [9] is a list up to topological equivalence. Four graphics with elliptic point appear in two forms (Figure 21) which in the blow-up are not topologically equivalent. The graphics appear in Figure 22.

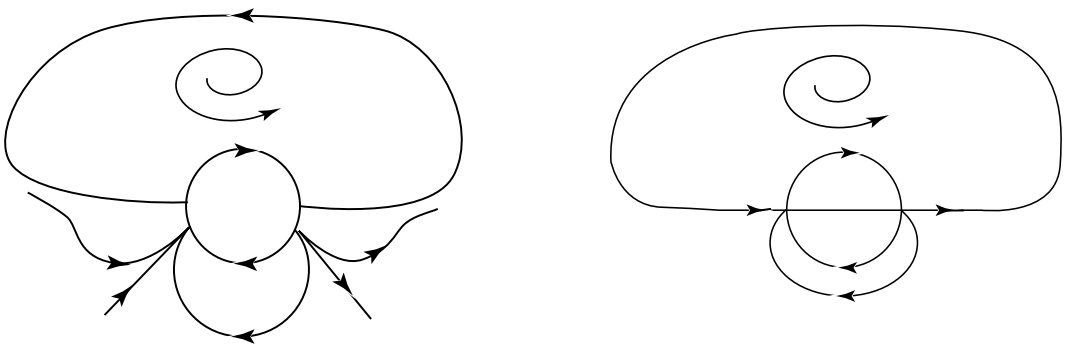

Figure 21: The two forms of an hh-graphic through an elliptic point

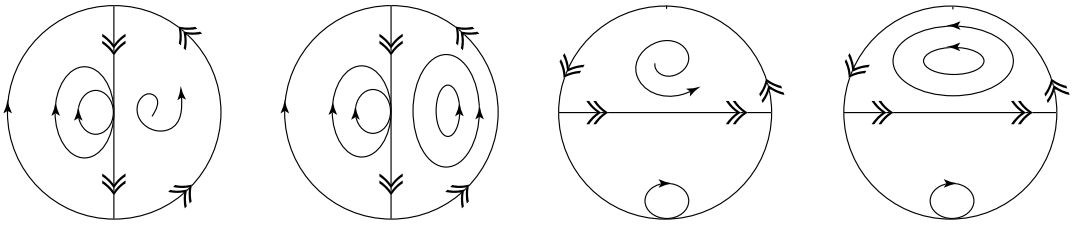

(a) (H_4^1) (b) (H_5^1) (c) (H_{12}^3) (d) (H_{13}^3)

Figure 22: The 4 additional cases

The Table 1 lists the different classes of graphics and what is done in each case.

Class of graphics	Done	Open but probably easy	Open
Hyperbolic graphics	10 (Mourtada)		
Elementary non hyperbolic graphics	47	1	
Graphics through a nilpotent saddle	2		2 (center cases)
Graphics through a nilpotent elliptic point with pp-transition	16		4 (center cases)
Graphics through a nilpotent elliptic point with hp-transition	6	4	
Graphics through a nilpotent elliptic point with hh-transition (mult. 3)	2	4	6 (center cases
The four additional cases			4
Graphics through a nilpotent elliptic point with multiplicity 4			4
Degenerate graphics			13
Total = 125	83	9	33

Table 1

The different classes will be discussed below together with references for proofs. The category "open but probably easy" is obviously subjective and reflects the belief of the author that no new methods but merely elementary calculations can allow to prove finite cyclicity. The calculations may not be short. The author has not checked all proofs. It is premature at this stage of the program, if we consider the fact that unifying proofs of many cases could appear before the program is completed.

Strategies to attack the program and avoid making mistakes.

(1) Start from the most generic graphics and follow by the more degenerate. As degenerate graphics bifurcate into generic graphics everything has to be coherent.

(2) Some graphics appear in families: the strategy is to study simultaneously all graphics in a family including the bordering graphics. Everything has to be coherent. Examples will be discussed below.

4.1 Hyperbolic graphics

Nearly all cases had been done, one by one, by elementary methods. More recently Mourtada announced

4.3 Theorem *([27], [28], [29], [30]) Any hyperbolic polycycle has finite cyclicity inside any analytic finite-parameter family of vector fields.*

When working with elementary methods the center cases are usually difficult problems. For instance the "triangle" (Figure 23) can lie at the intersection of 3 strata: indeed it has 3 invariant lines, yielding Darboux integrability. It can be time-reversible when there is a symmetry axis and it can simultaneously be Hamiltonian.

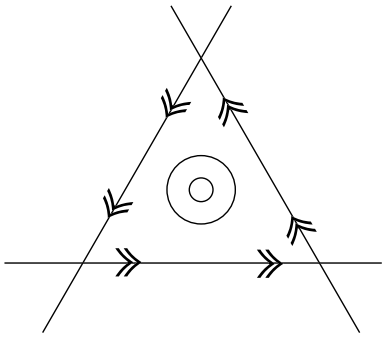

Figure 23: The triangle

4.2 Elementary non-hyperbolic graphics

4.4 Definition A graphic is *elementary* if all its singular points are *elementary* (i.e. with one or 2 nonzero eigenvalues), either hyperbolic saddles or *semi-hyperbolic points* (i.e. points with exactly one zero eigenvalue).

The finite cyclicity of these graphics are usually easier problems and all graphics are treated with elementary methods.

- The case (I^2_{13}) is treated in [41].
- 46 cases are treated in different papers to which the author contributed: [10], [6], [7], [35].

- the graphic (I^2_{16a}) is still open.

Ingredients used.

(1) C^k normal forms near the saddle-nodes

$$\begin{array}{rcl} \dot{x} & = & x^2+\epsilon \\ \dot{y} & = & \pm y(1+ax) \end{array} \tag{4.5}$$

and semi-hyperbolic saddles

$$\begin{array}{rcl} \dot{x} & = & x^3+\epsilon_2 x+\epsilon_1 \\ \dot{y} & = & -y(1+ax^2). \end{array} \tag{4.6}$$

It is remarkable that the C^k normal forms have been sufficient even in the center cases!

(2) We have two types of transition maps near a semi-hyerbolic point:

- **Central transition** (Figure 24a). The Dulac map is linear when it exists (it does not exist for $\epsilon = 0$!):

$$D_\epsilon(y) = m(\epsilon)y, \qquad \lim_{\epsilon\to 0} m(\epsilon) = 0. \tag{4.7}$$

- **Stable-center transition** (Figure fig24b). The Dulac map D_ϵ is flat in (x,ϵ) and has additional flatness properties [10].

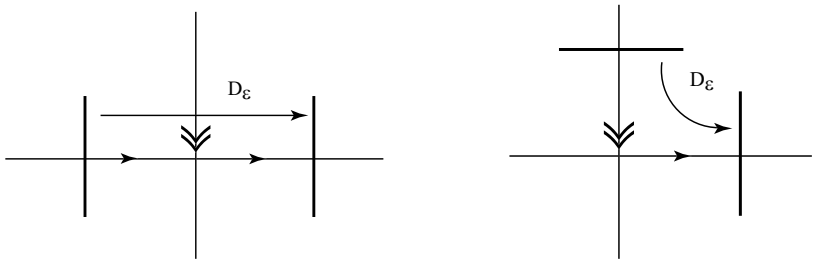

(a) central transition (b) stable-center transition

Figure 24: The Dulac maps for a saddle-node

(3) Khovanskii's method is used as soon as the Poincaré return map contains the composition of a stable-center transition with a center-unstable transition. The principle of *Khovanskii's method* is that the Dulac map is a solution of a Pfaff equation:

- **Case of a central transition.** The Pfaff equation is:

$$xdy - ydx = 0. \tag{4.8}$$

- **Case of a stable-center (center-unstable) transition.** The Pfaff equation is:

$$F(x)dy \mp ydx = 0, \tag{4.9}$$

where the normal form is

$$\begin{array}{rcl} \dot{x} & = & F(x) \\ \dot{y} & = & \mp y \end{array} \tag{4.10}$$

(4) Except for (I^2_{13}) which is treated in [41] all center cases are not located at the intersection of strata of centers: the *Bautin ideal* is radical allowing an elementary treatment [35].

Hence:

- we first make a proof in the generic case (e.g. (I^2_4), Figure 25a);
- we then transform it into a proof for the center case by a Bautin type argument (e.g. (I^2_5), Figure 25b).

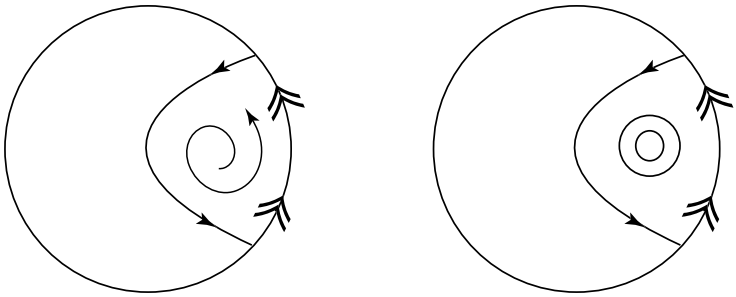

(a) (I^2_4) (b) (I^2_5)

Figure 25: The graphics (I^2_4) and (I^2_5)

The left open case (I^2_{16a}). There is a continuum of graphics (I^2_{16a}) (Figure 26): they occur inside a family.

The bordering graphic (I^2_{16b}) is treated in [35] and (H^3_6) is treated in [7]. Moreover a proof of finite cyclicity is given in [7] for the corresponding generic graphics (I^2_{14a}) and (I^2_{15a}) appearing when breaking the center condition. As the Bautin ideal is radical we "should" be able, with mere calculations, to reduce the center case to the generic case via a Bautin type argument.

We still believe that such calculations can be done, but that they will take more than one or two pages.

A remark on the genericity condition used to make the proof in the generic cases. Note that any of the graphics (I^2_{14a}), (I^2_{15a}) and (I^2_{16a}) is of the form appearing in Figure 27. We take sections near the singular points as in Figure 27 and calculate the different Dulac maps in the neighborhood of the singular points and regular transitions.

The sections are taken in normalizing C^k normal forms in the neighborhood of the singular points allowing an explicit calculation of the Dulac maps. In all the discussion λ is the multi-parameter of the problem and we suppose that the graphic occurs at $\lambda = 0$. We discuss the

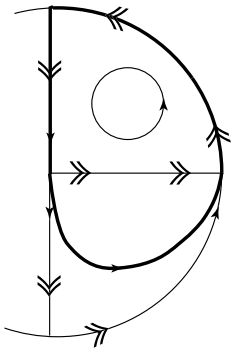

Figure 26: The graphic (I_{16a})

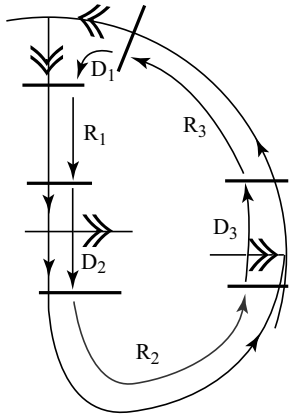

Figure 27: The transition maps for (I^2_{14a}), (I^2_{15a}) and (I^2_{16a})

easier case, namely the one where the hyperbolicity ratio at P_1 is $r(0)$, with $r(0)$ irrational (the other cases are similar but a little longer to write). Then the normal form near P_1 is

$$\begin{array}{rcl} \dot{x}_1 & = & x_1 \\ \dot{y}_1 & = & -r(\lambda)y_1 \end{array} \tag{4.11}$$

Moreover we have

$$D_2(x_2) = M(\lambda)x_2, \qquad \lim_{\lambda\to 0} M(\lambda) = +\infty, \tag{4.12}$$

$$D_3(x_3) = m(\lambda)x_3, \qquad \lim_{\lambda\to 0} m(\lambda) = 0. \tag{4.13}$$

It is shown in [16] that the C^k-changes of coordinates to normal form are not unique. Using this freedom allows to simplify the regular transitions. Because the connection along the equator is fixed we can suppose that R_3 is the identity and $R_1(y_1) = y_1 + \delta$ is a translation. Hence the Poincaré return map is identically zero for some λ if

$$R_{2,\lambda}(x_3) = \left[m(\lambda)^{-1/r(\lambda)} M(\lambda)^{-1} x_3 - \delta\right]^{1/r(\lambda)}, \tag{4.14}$$

i.e. $R_{2,\lambda}$ is the $1/r$-th power of an affine map. A generic condition on $R_{2,0}$ for $\lambda = 0$ is that$R_{2,0}$ is not the $1/r$-th power of an affine map at the level of a finite jet.

How to check this condition in practice? A simple method, *the analytic extension principle,* exists because we deal with analytic vector fields. Indeed our graphic occurs in a family of graphics. Let us look near the boundary graphic which is the hemicycle (Figure 28). The transition maps f and g along the invariant line and the equator are nonlinear as soon as the hyperbolicity ratio of the point P_4 is different from 1.

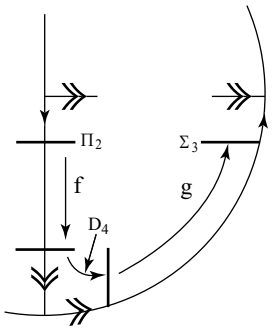

Figure 28: The lower part of the hemicycle

Indeed in [7] we showed through an explicit calculation that f and g have a non-vanishing second derivative. In the particular case where the hyperbolicity ratio is equal to 1 it is possible to prove that P_4 is non-integrable (the first saddle quantity is nonzero).

- So graphics very close to the hemicycle verify the genericity condition.
- The analycity extension principle guarantees that we can choose the sections Π_2 and Σ_3 analytic and parametrized by analytic coordinates. Hence we can "push" the genericity condition to the whole family of graphics.

The analycity extension principle lies on the following theorems proved in [8].

4.5 Theorem *A saddle-node of an analytic vector field can be brought in the neighborhood of the origin to the normal form*

$$\begin{aligned} \dot{x} &= x^2 \\ \dot{y} &= \pm y(1+ax) \end{aligned} \tag{4.15}$$

by a C^∞ change of coordinates which is analytic outside $x = 0$.

4.6 Theorem *For a C^∞ unfolding of a germ of analytic vector field with a saddle-node at the origin there exists a finitely smooth orbital equivalence with the polynomial normal form*

$$\begin{aligned} \dot{x} &= x^2 - \epsilon \\ \dot{y} &= \pm y(1+ax). \end{aligned} \tag{4.16}$$

For $\epsilon = 0$ this equivalence is analytic outside the strong manifold.

4.3 Graphics through a nilpotent saddle

4.7 Theorem *(Zhu [40]) A "convex" graphic through a nilpotent saddle of codimension 3 (Figure* 29*) has finite cyclicity if the return map has a derivative different from 1.*

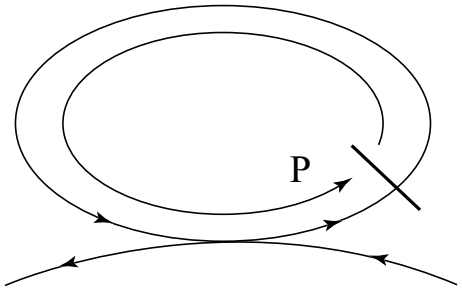

Figure 29: A "convex" graphic through a nilpotent saddle

The two cases appearing in Figure 30 have been shown to have finite cyclicity:

- the transition occurs along an invariant parabola allowing to calculate $P'(0)$.
- A few adjustments to the proof allow to treat the case with an additional saddle-node.
- The point can be of codimension 4, but the transition is fixed along the equator so the proof of the theorem 4.7 can be easily adjusted to this case.

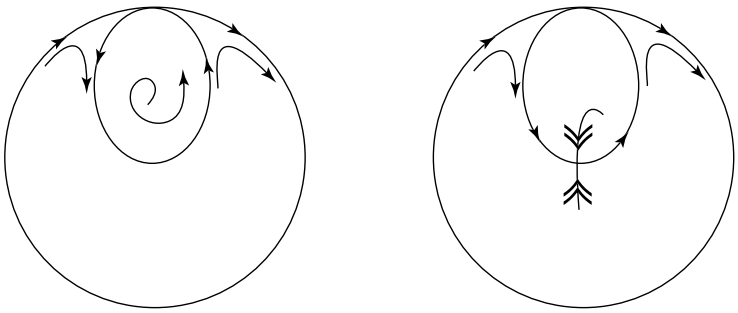

(a) (I^1_{12}) (b) (I^1_{13})

Figure 30: The two graphics with nilpotent saddle and finite cyclicity

The two cases which remain to be done are two center cases. Moreover they can lie at the intersection of strata of centers.

4.4 The 3 types of transition through an elliptic nilpotent point of multiplicity 3

They appear in Figure 31: on the left we draw the graphics. On the right the same graphics are drawn when the elliptic point has been blown up. They are called pp-graphic (resp. hp-graphic, hh-graphic) using the names of [23]. In the names "p" refers to a parabolic sector and "h" to a hyperbolic sector. Hence an hp graphic starts between two hyperbolic sectors to end in a parabolic sector.

4.8 Theorem *(Zhu [40]) A graphic through a nilpotent elliptic point of multiplicity 3 has finite cyclicity under one of the following conditions:*

- **hp-graphic***: no condition;*
- **pp-graphic***: the transition map in normal coordinates near the singular points on the blow-up circle (Figure* 32*) is nonlinear;*
- **hh-graphic***: the point is of codimension 3 and the return map has a derivative different from 1.*

We will discuss the fact that the hypotheses which look so different for the 3 cases are indeed consistent.

Consistency of the hypotheses.

- An hp-graphic contains pp-graphics in its neighborhood and can bifurcate into a pp-graphic. All these pp-graphics satisfy the genericity condition. This comes from the nonlinearity of the passage from Σ to Π in Figure 33.
- Similarly an hh-graphic can bifurcate into hp- and pp-graphics. The pp-graphics produced are generic because the two passages from Σ_i to Π_i in Figure 34 are nonlinear and nearly symmetric one to the other. The transition map from Π_2 to Π_1 remains nonlinear (there is no compensation) as $P'(0) \neq 1$.

What remains to be done for quadratic systems? Essentially to adapt the proof of Theorem 4.8 when either the nilpotent point is of multiplicity four or there are additional singular points on the graphics: up to two hyperbolic saddles and/or one saddle-node.

Case of pp-graphics

- All adaptations have been done in [36] for the graphics with extra singular points and not surrounding a center.
- Four center cases remain to be done.

Case of hp-graphics

- Adaptations to the graphics with an extra saddle-node have been done.

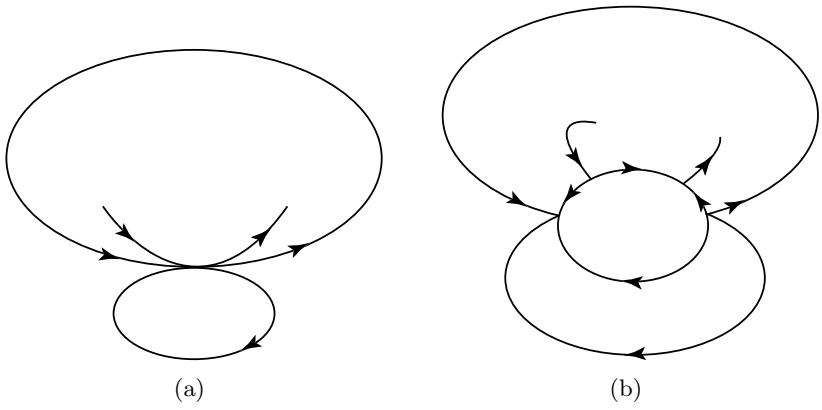

(a) (b)

pp-graphics

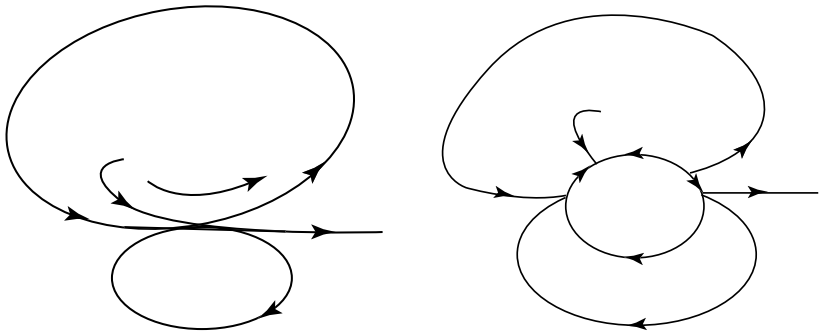

(c) (d)

hp-graphics

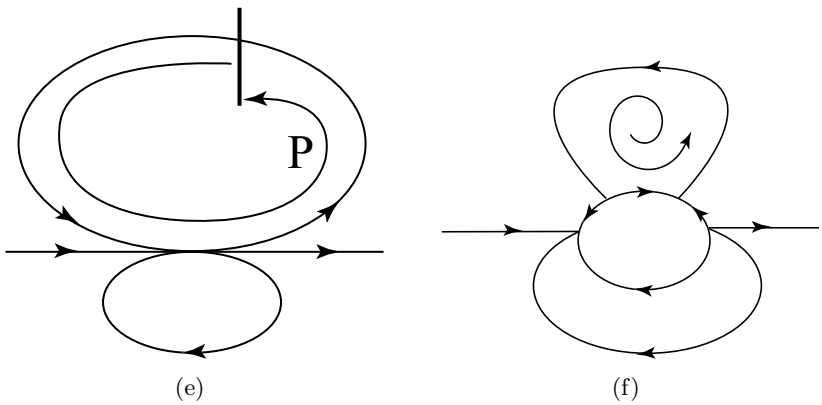

(e) (f)

hh-graphics

Figure 31: The three types of graphics through an elliptic point

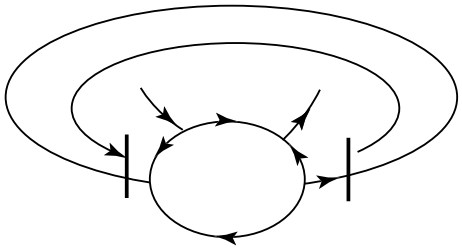

Figure 32: A pp-graphic

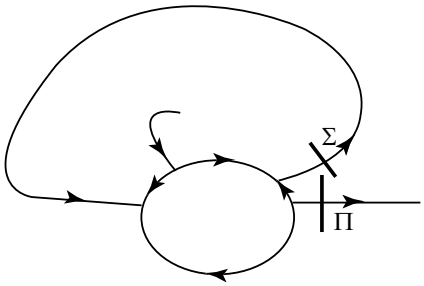

Figure 33: Nonlinearity of the passage from Σ to Π

- Adaptations to the graphics with an extra saddle remain to be done. If the saddles have had a hyperbolicity ratio $r < 1$ the adaptation would have been a few lines. In quadratic systems we always have the bad case $r > 1$. We still hope to solve the 4 remaining cases with mere calculations.

Case of hh-graphics

- As for graphics through a nilpotent saddle, the transition occurs along an invariant parabola, allowing to calculate $P'(0)$.
- An adaptation is needed for the codimension 4 case. The codimension 4 type I corresponds to $\epsilon = 0$, $b > 2\sqrt{2}$, in the normal form

$$\begin{array}{rcl} \dot{x} & = & y \\ \dot{y} & = & -x^3 + bxy + \epsilon x^2 y + o(|x,y|^5). \end{array} \tag{4.17}$$

  The condition $\epsilon \neq 0$ was used to show that the transition maps of Figure 35 are nonlinear.

  For quadratic systems with $\epsilon = 0$ the four singular points on the blow-up circle are non integrable as soon as $P'(0) \neq 1$, hence we believe that the proofs can be adapted.

- An adaptation is needed for hemicycles (2 extra saddles) (Figure 36) with the nilpotent point on the invariant line or at infinity. We may have an additional saddle-node.
- The center cases have to be done.

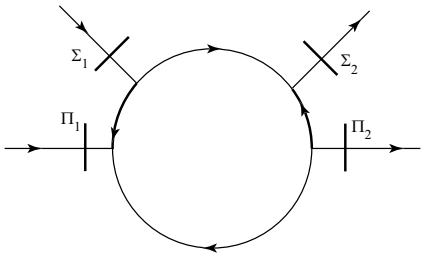

Figure 34: The passage from Σ_i to Π_i

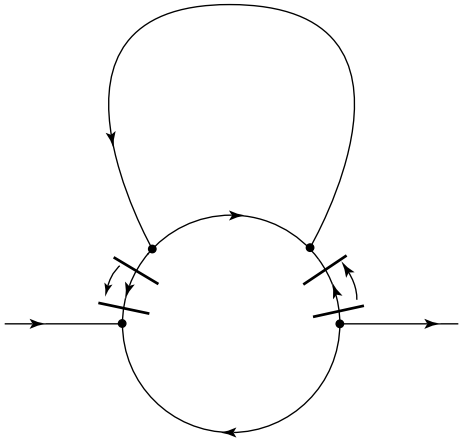

Figure 35: The two transition maps along arcs of the blow-up circle

4.5 The four additional cases

These are four graphics with a nilpotent elliptic point of codimension 4 type II ($b = 2\sqrt{2}$ in (4.17)) (see Figure 37).

A priori we could expect the generic cases to be treated by the standard technique of the blow-up of the family.

As we work in quadratic systems and the nilpotent focus does not exist in quadratic systems (there is a fold in parameter space) we can take the following family as a normal form near the elliptic point

$$\begin{aligned} \dot{x} &= y + (\tfrac{1}{2} + \mu_4)x^2 + \mu_2 \\ \dot{y} &= \mu_1 + \mu_3 y + xy \end{aligned} \tag{4.18}$$

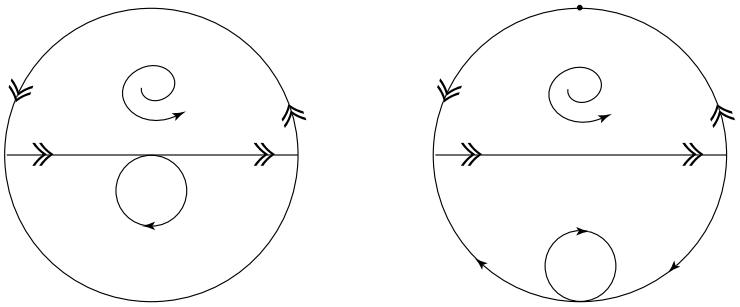

(a) (H_4^1) (b) (H_8^3)

Figure 36: The graphics (H_4^1), (H_8^3)

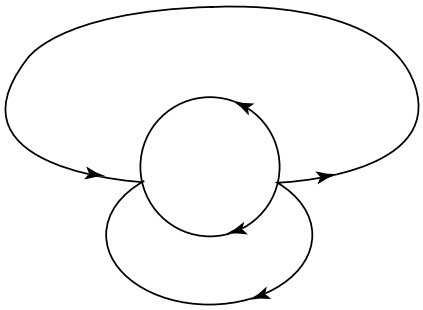

Figure 37: The type of the 4 additional cases

The blow-up of the family is the following

$$\begin{cases} x = r\overline{x} \\ y = r^2\overline{y} \\ \mu_1 = r^3\rho^3\overline{\mu}_1 \\ \mu_2 = r^2\rho^2\overline{\mu}_2 \\ \mu_3 = r\rho\overline{\mu}_3, \end{cases} \tag{4.19}$$

$(\overline{x}, \overline{y}, \rho) \in S^2$, $(\overline{\mu}_1, \overline{\mu}_2, \overline{\mu}_3) \in S^2$, r, μ_4 small.

4.6 The graphics with a nilpotent point of multiplicity 4 and the degenerate graphics

Nilpotent points of multiplicity 4 have a normal form

$$\begin{aligned} \dot{x} &= y \\ \dot{y} &= x^4 + bxy + \dots \end{aligned} \tag{4.20}$$

Degenerate graphics have one or two lines of singular points.

A priori we expect that the method of the blow-up of the family adapted by Dumortier and Roussarie ([11] and [12]) for the Canard cycles can work for the generic cases. But the

blow-up will generate lines of singular points in the blown-up family. So even for the graphics with a nilpotent point of multiplicity 4 we expect to apply the methods developed to study singular perturbations.

4.7 The status of all graphics

For the sake of completeness we have added the status of all graphics of the family. The names refer to the grahics of [9].

Graphics done.

- Hyperbolic graphics: (F_1^1), (F_2^1), $F_2^2)$, (F^3), (H_1^1), (H_2^1), (I_1^2), (I_2^2), (I_6^2), (I_7^2)
- Semi-hyperbolic graphics: (F_2^1), (F_3^1), (F_4^1), (F_3^2), (F_4^2), (H_3^1), (H_8^1), (H_9^1), (H_{10}^1), (H_{11}^1), (H_{12}^1), (I_3^2), (I_4^2), (I_5^2), $I_8^2)$, (I_9^2), (I_{10}^2), (I_{11}^2), (I_{12}^2), (I_{13}^2), (H_1^3), (H_2^3), (H_3^3), (H_4^3), (I_{14a}^2), (I_{14b}^2),(H_5^3), (I_{15a}^2), (I_{15b}^2), (H_6^3), (I_{16a}^2), (I_{19}^2), (I_{20}^2), (I_{21}^2), (I_{22}^2), (I_{27}^2), (I_{28}^2), (I_{29}^2), (I_{30}^2), (I_{31}^2), (I_{32}^2), (I_{33}^2), (I_{34}^2), (I_{35}^2), (I_{36}^2), (I_{37}^2), (I_{38}^2)
- Graphics with a nilpotent saddle: (I_{12}^1), (I_{13}^1)
- pp-graphics with a nilpotent elliptic point: (H_6^1), (F_{6a}^1), (H_7^3), (I_{17a}^2), (H_9^3), (I_{5a}^1), (H_{10}^3), (I_{18a}^2), (I_{23}^2), (I_{7a}^1), (I_{24}^2), (I_{8a}^1), (I_{25}^2), (I_{9a}^2), (I_{39}^2), (I_{10a}^1)
- hp-graphics with a nilpotent elliptic point: (F_{6b}^1), (I_{5b}^1), (I_{7b}^1), (I_{8b}^1), (I_{10b}^1), (I_{11a}^1)
- hh-graphics with a nilpotent elliptic point: (I_{9b}), (I_{11b}^1)

Graphics to be done and probably easy.

- Semi-hyperbolic graphic: (I_{16a}^2)
- hp-graphics with a nilpotent elliptic point: (I_{17b}^2), (I_{18b}^2), (I_{26}^2), (I_{40}^2)
- hh-graphics with a nilpotent elliptic point: (H_4^1), (H_8^3), (H_{12}^3), (H_{15}^3)

Open cases.

- Graphics with a nilpotent saddle: (F_5^1), (I_{14}^1)
- pp-graphics with a nilpotent elliptic point: (H_7^1), (F_{7a}^1), (H_{11}^3), (I_{6a}^1)
- hh-graphics with a nilpotent elliptic point: (H_5^1),(F_{7b}^1), (H_{13}^1), (I_{6b}^1), (H_{13}^3), (H_{14}^3)
- The four additional cases: (H_4^1), (H_5^1), $H_{12}^3)$, (H_{13}^3)
- Graphics with a nilpotent point of multiplicity 4: (I_1^1), (I_2^1), (I_3^1), (I_4^1)
- Degenerate graphics: (DH_1), (DF_{1a}), (DF_{1b}), (DH_2), (DF_{2a}), (DF_{2b}), (DH_3), (DF_{3a}), (DF_{3b}), (DH_4), (DF_{4a}), (DF_{4b}), (DH_5).

References

[1] L. Sylow, and S. Lie, *Œuvres complètes de Niels Henrik Abel*, Christiana, Imprimerie de Grøndlhal & Son, Johnson Reprint Corporation, 1965.

[2] R. Bamon, Quadratic vector fields in the planr have a finite number of limit cycles, *Inst. Hautes Etudes Sci. Publ. Math* **64** (1986), 111–142.

[3] L. Cairo, H. Giacomini, and J. Llibre, Liouvillian first integrals for the planar Lotka-Volterra system, preprint, (2002).

[4] C. Christopher, and C. Rousseau, Normalizable, integrable and linearizable saddle points in the Lotka-Volterra system, preprint CRM (2002).

[5] C. Christopher, P. Mardešić, and C. Rousseau, Normalizable, integrable and linearizable points in complex quadratic systems in C^2, preprint CRM (2002), to appear in J. Dynam. and Control Syst.

[6] F. Dumortier, M. El Morsalani, and C. Rousseau, Hilbert's 16th problem for quadratic systems and cyclicity of elementary graphics, *Nonlinearity* **9** (1996), 1209-1261.

[7] F. Dumortier, A. Guzmán, and C. Rousseau, Finite cyclicity of elementary graphics surrounding a focus or center in quadratic systems, *Qual. Theory Dynam. Syst.*, under press.

[8] F. Dumortier, Y. Ilyashenko, and C. Rousseau, Normal forms near a saddle-node and applications to the finite cyclicity of graphics, *Ergod. Theor. Dyn. Systems* **22** (2002), 783–818.

[9] F. Dumortier, R. Roussarie, and C. Rousseau, Hilbert's 16-th problem for quadratic vector fields, *J. Differential Equations* **110** (1994), 86–133.

[10] F. Dumortier, R. Roussarie, and C. Rousseau, Elementary graphics of cyclicity 1 and 2, *Nonlinearity* **7** (1994), 1001–1043.

[11] F. Dumortier, and R. Roussarie, Canard cycles and center manifolds. With an appendix by Chengzhi Li, *Mem. Amer. Math. Soc.* **121** (1996), no. 577.

[12] F. Dumortier, and R. Roussarie, Multiple canard cycles in generalized Liénard equations, *J. Differential Equations* **174** (2001), 1–29.

[13] J. Ecalle, *Les fonctions résurgentes*, Publications mathématiques d'Orsay, 1985.

[14] A. Fronville, A. Sadovski, and H. Żołądek, Solution of the 1:-2 resonant center problem in the quadratic case, *Fundamenta Mathematicae* **157** (1998) 191–207.

[15] A. A. Glutsyuk, Confluence of singular points and nonlinear Stokes phenomenon, *Trans. Moscow Math. Soc.*, **62** (2001), 49–95.

[16] A. Guzmán, and C. Rousseau, Genericity conditions for finite cyclicity of elementary graphics, *J. Differential Equations* **155** (1999), 44–72.

[17] S. Gravel and P. Thibault, Integrability and linearizability of the Lotka-Volterra system for $\lambda \in Q$, *J. Differential Equations* **184** (2002), 20–47.

[18] H. Hukuhara, T. Kimura, and T. Matuda, *Équations différentielles ordinaires du premier ordre dans le champ complexe*, Math. Soc. of Japan, 1961.

[19] Y. Ilyashenko, Divergence of series reducing an analytic differential equation to linear normal form at a singular point, *Funct. Anal. Appl.*, **13** (1979), 227–229.

[20] Y. Ilyashenko, In the theory of normal forms of analytic differential equations, divergence is the rule and convergence the exception when the Bryuno conditions are violated, *Moscow University Mathematics Bulletin*, **36** (1981) 11–18.

[21] Y. Ilyashenko, Nonlinear Stokes phenomena, in *Nonlinear Stokes phenomena*, Y. Ilyashenko editor, Advances in Soviet Mathematics, vol. 14, Amer. Math. Soc., Providence, RI, (1993), 1-55.

[22] Y.S. Ilyashenko, and A.S. Pyartli, Materialization of Poincaré resonances and divergence of normalizing series, *J. Sov. Math.* **31** (1985), 3053–3092.

[23] A. Kotova, and V. Stanzo, On few-parameter generic families of vector fields on the two-dimensional sphere, in *Concerning the Hilbert's problem*, Amer. Math. Soc. Trans. Ser. 2, **165**, AMS, Providence, RI, (1995), 155-201.

[24] P. Lavaurs, Systèmes dynamiques holomorphes: explosion de points périodiques paraboliques, Ph.D. Thesis, Université de Paris-Sud, 1989.

[25] O. Lehto, Quasi-conformal mappings in the plane, *N.Y. Springer*, 1973.

[26] J. Martinet, Remarques sur la bifurcation nœud-col dans le domaine complexe, *Astérisque* **150-151** (1987), 131–149.

[27] A. Mourtada, Projection de sous-ensembles quasi-réguliers de Dulac-Hilbert. Un cas nœthérien, prépublication, Laboratoire de Topplogie, Université de Bourgogne (1997).

[28] A. Mourtada, Projection de sous-ensembles quasi-réguliers d'Hilbert II, prépublication, Laboratoire de Topplogie, Université de Bourgogne (1999).

[29] A. Mourtada, Projection de sous-ensembles quasi-réguliers d'Hilbert III, prépublication, Laboratoire de Topplogie, Université de Bourgogne (2001).

[30] A. Mourtada, Projection de sous-ensembles quasi-réguliers d'Hilbert IV: le cas général, prépublication, Laboratoire de Topplogie, Université de Bourgogne (2002).

[31] J.-F. Mattei, and R. Moussu, Holonomie et intégrales premières, *Ann. Scient. Éc. Norm. Sup.*, 4^e série **13** (1980), 469–523.

[32] J. Martinet, and J.-P. Ramis, Problèmes de modules pour des équations différentielles non linéaires du premier ordre, *Publ. Math., Inst. Hautes Etud. Sci.* **55** (1982), 63–164.

[33] P. Mardešić, R. Roussarie and C. Rousseau, Modulus of analytic classification for unfoldings of generic parabolic diffeomorphisms, preprint CRM (2002).

[34] R. Pérez-Marco, and J.-C. Yoccoz, Germes de feuilletages holomorphes à holonomie prescrite, *Astérisque* **222** (1994), 345–371.

[35] C. Rousseau, G. Świrszcz, and H. Żołądek, Cyclicity of graphics with semi-hyperbolic points inside quadratic systems, *J. Dynam. Control Systems* **4** (1998), 149–189.

[36] C. Rousseau, and H. Zhu, PP-graphics with a nilpotent elliptic singularity in quadratic systems and Hilbert's 16th problem, preprint CRM (2002).

[37] M. Shishikura, Bifurcations of parabolic fixed points, in *The Mandelbrot set, theme and variations*, Tan Lei Editor, London Math. Soc. Lecture Note Ser., **274**, Cambridge Univ. Press, Cambridge, 2000, 325–363.

[38] S. M. Voronin, Analytic classification of germs of conformal maps $(C,0) \to (C,0)$ with identical linear part, *Funct. Anal. Appl.* **16** (1982).

[39] J.-C. Yoccoz, Théorème de Siegel, nombres de Bruno et polynômes quadratiques, *Astérisque* **231** (1995),1–88.

[40] H. Zhu, and C. Rousseau, Finite cyclicity of graphics through a nilpotent singularity of elliptic or saddle type, *J. Differential Equations* **178** (2002), 325-436.

[41] H. Żołądek, The cyclicity of triangles and segments in quadratic systems, *J. Differential Equations* **122** (1995), 137–159.